

Division of Molecular Structural Biology
Department of Medical Biochemistry and Biophysics
Karolinska Institutet, Stockholm, Sweden

STRUCTURAL ENZYMOLOGY OF OXALATE DEGRADATION IN *OXALOBACTER FORMIGENES*

Catrine L. Berthold



**Karolinska
Institutet**

Stockholm 2007

All previously published papers were reproduced with permission from the publisher.

Published by Karolinska Institutet. Printed by Intellecta DocuSys AB

© Catrine L. Berthold, 2007

ISBN 978-91-7357-409-9

ABSTRACT

Oxalic acid, as one of nature's most highly oxidised compounds, is toxic to most organisms. It is introduced in the human body in the diet but also as a waste product of cellular metabolism. Mammals do not possess the ability to degrade oxalate and must excrete it in the urine or through the intestine. Accumulation of oxalate may lead to a number of pathological conditions in humans and a majority of all kidney stones are formed by calcium oxalate. Fortunately, the anaerobic bacterium *Oxalobacter formigenes* has been shown to play a key role in the mammalian oxalate homeostasis. The bacterium, which inhabits the gastrointestinal tract of most vertebrates including humans, has evolved a method for oxalate catabolism and degrades it in a two enzyme pathway releasing formate and carbon dioxide.

This thesis presents structural characterisation of the two enzymes active in oxalate catabolism in *O. formigenes*, oxalyl-CoA decarboxylase (OXC) and formyl-CoA transferase (FRC). FRC catalyses the activation of oxalate in the form of oxalyl-CoA by transferring a CoA carrier from formyl-CoA. OXC, the second enzyme of the pathway, decarboxylates oxalyl-CoA releasing carbon dioxide and regenerating formyl-CoA.

The three-dimensional structure of OXC was determined to 1.73 Å resolution from a merohedrally twinned crystal. As a thiamin diphosphate-dependent enzyme, OXC displays the conserved fold consisting of three α/β -domains with the coenzyme bound in a strictly conserved conformation between two subunits. A novel set of active site residues was observed for OXC, and the identification of an ADP molecule bound in the regulatory domain of the protein led to the discovery that ADP is an efficient activator of OXC. Several structures of OXC complexes have been determined, including a substrate complex with an inactive coenzyme analogue, a product complex and a reaction intermediate obtained by freeze-trapping experiments. A catalytic mechanism is presented based on a combination of structural features and mutagenesis data.

FRC, as a Class III CoA-transferase, is a homodimeric enzyme with a peculiar fold consisting of two monomers interlocking each other like links of a chain. By freeze-trapping crystallography we have identified a previously undiscovered intermediate in the catalytic reaction of FRC, leading to reinterpretation of the catalytic mechanism. Active site features in structures of several reaction intermediates and point-mutated variants are combined to present a plausible scenario for the catalytic steps. Finally, we demonstrate that a protein annotated as a putative formyl-CoA transferase in *Escherichia coli* is indeed a FRC ortholog, and the substrate specificity and kinetic behaviour of the two enzymes are compared.

LIST OF PUBLICATIONS NOT INCLUDED IN THESIS

- Berthold CL, Gocke D, Pohl M and Schneider G. Crystal structure of the branched-chain keto acid decarboxylase (KdcA) from *Lactococcus lactis*; structural basis for the broad substrate spectra accepted for carboligation. *Acta Crystallographica*. 2007; D63: 1217–1224
- Gocke D, Walter L, Gauchenova K, Kolter G, Knoll M, Berthold CL, Schneider G, Pleiss J, Müller M and Pohl M. Accessing (S)-2-hydroxy ketones by rational protein design of ThDP-dependent enzymes. Accepted for publication in *ChemBioChem*.
- Gocke D, Berthold CL, Graf T, Brosi H, Frindi-Wosch I, Knoll M, Stillger T, Walter L, Müller M, Pleiss J, Schneider G and Pohl M. Pyruvate Decarboxylase from *Acetobacter pasteurianus*: Biochemical and structural characterisation. Submitted to *Protein Engineering, Design and Selection*.
- Ågren D, Stehr M, Berthold CL, Kapoor S, Oehlmann W, Singh M, and Schneider G. Three-dimensional structure of apo- and holo L-alanine dehydrogenase from *Mycobacterium tuberculosis* reveal conformational changes upon coenzyme binding. Submitted to *Journal of Molecular Biology*.

LIST OF PUBLICATIONS

- I. Berthold CL, Sidhu H, Ricagno S, Richards NG and Lindqvist Y. Detection and characterization of merohedral twinning in crystals of oxalyl-coenzyme A decarboxylase from *Oxalobacter formigenes*. *Biochimica et Biophysica Acta*. 2006; 1764:122-128.
- II. Berthold CL, Moussatche P, Richards NGJ and Lindqvist Y. Structural basis for activation of the thiamin diphosphate-dependent enzyme oxalyl-CoA decarboxylase by adenosine diphosphate. *Journal of Biological Chemistry*. 2005; 280(50): 41645-41654.
- III. Berthold CL, Toyota CG, Moussatche P, Wood MD, Leeper F, Richards NGJ and Lindqvist Y. Crystallographic snapshots of oxalyl-CoA decarboxylase give insights into catalysis by non-oxidative ThDP-dependent decarboxylases. *Structure*. 2007; 15: 853-861.
- IV. Berthold CL, Toyota CG, Richards NGJ and Lindqvist Y. Re-investigation of the catalytic mechanism of formyl-CoA transferase, a Class III CoA-transferase. Submitted to *Journal of Biological Chemistry*.
- V. Toyota CG, Berthold CL, Guez A, Jónsson S, Lindqvist Y, Cambillau C and Richards NGJ. Differential substrate specificity and kinetic behavior in *Escherichia coli* YfdW and *Oxalobacter formigenes* Formyl-CoA transferase. Submitted to *Journal of Bacteriology*.

LIST OF ABBREVIATIONS

OXC	Oxalyl-coenzyme A decarboxylase from <i>Oxalobacter formigenes</i>
FRC	Formyl-coenzyme A transferase from <i>Oxalobacter formigenes</i>
OxIT	Oxalate:formate antiporter
ThDP	Thiamin diphosphate
ThTDP	Thiamin-2-thiazolone diphosphate
dzThDP	3'-deaza thiamin diphosphate
ADP	Adenosine diphosphate
CoA	Coenzyme A
ACP	Acyl-carrier protein
YfdW	FRC ortholog in <i>Escherichia coli</i> coded by the <i>yfdw</i> gene
CaiB	γ -butyrobetaine-CoA:carnitine CoA transferase
PEG	Polyethylene glycol
MES	4-morpholineethane sulfonic acid
HEPES	4-(2-hydroxyethyl)-1-piperazineethane sulfonic acid
Bis-Tris Propane	2-[bis(2-hydroxyethyl)amino]-2-(hydroxymethyl)propane-1,3,-diol
FPLC	Fast protein liquid chromatography
HPLC	High performance liquid chromatography

CONTENTS

1	General Introduction	1
1.1	Enzymes and Structural enzymology	1
1.2	Aim of thesis	2
1.3	Oxalate homeostasis	3
1.3.1	Oxalate.....	3
1.3.2	<i>Oxalobacter formigenes</i>	4
1.3.3	Oxalate catabolism.....	4
2	Oxalyl-CoA Decarboxylase- A <i>Thiamin Diphosphate Dependent Enzyme</i>	7
2.1	Thiamin history	7
2.2	Thiamin diphosphate.....	7
2.2.1	The coenzyme	8
2.3	Thiamin diphosphate dependent enzymes	8
2.3.1	The five subfamilies.....	9
2.3.2	Subunit architecture and oligomeric state	11
2.3.3	Coenzyme binding	12
2.3.4	Coenzyme activation.....	13
2.4	Thiamin diphosphate dependent decarboxylation	14
2.4.1	Decarboxylation	15
2.4.2	The α -carbanion/enamine intermediate	15
2.4.3	Product formation and release	15
2.5	Results on oxalyl-CoA decarboxylase	15
2.5.1	Crystallisation and structure determination (Paper I)	16
2.5.2	Structure of the holoenzyme (Paper II)	16
2.5.3	Crystallographic snapshots (Paper III)	18
2.5.4	Concluding remarks on oxalyl-CoA decarboxylase	21
3	Formyl-CoA Transferase- A <i>Class III Coenzyme A Transferase</i>	23
3.1	The thioester bond and coenzyme A	23
3.1.1	Structure of coenzyme A	23
3.1.2	Binding of coenzyme A in proteins.....	24
3.2	Coenzyme A transferases	24
3.2.1	Class I.....	25
3.2.2	Class II.....	26
3.2.3	Class III	26
3.2.4	Formyl-CoA transferase- Background	27
3.3	Results on formyl-CoA transferase	29
3.3.1	Reinvestigation of the catalytic mechanism (Paper IV)	29
3.3.2	Comparison with the <i>E. coli</i> ortholog (Paper V).....	34
3.3.3	Concluding remarks on formyl-CoA transferase	35
4	References	36
5	Acknowledgements	44

1 GENERAL INTRODUCTION

1.1 ENZYMES AND STRUCTURAL ENZYMOLOGY

As one of the major classes of macromolecules in all living systems, proteins perform and control most of the chemical processes necessary for life. By taking the role of catalysts, the enzymes enhance the rate of specific chemical reactions and control the reaction paths carefully in order to prevent undesired side reactions. Enzymes accomplish this by various means but all by lowering the activation energy of the conversion from reactants to products. Through evolution nature has created a fine tuned system where enzymes play a central role by regulating and performing the chemistry of life.

There are two major factors to consider regarding enzymes and their functions. First of all the substrate binding and specificity is of central importance. The arrangement of functional groups in the enzyme's active site has an important role here and there are often very precise interactions between the amino acid residues and the substrate that render what substrates the enzyme can accept.

Formation of the enzyme-substrate complex and alignment of the substrate for catalysis might require transient reorganizations of the active site or even larger parts of the enzyme. There are numerous enzymes where conformational changes of loops or even domains take place in order to accommodate the substrate or to create tunnels for substrate or product transport. Binding of substrates commonly also induce the active conformation of the enzyme, where the structure arranges into the form active for catalysis.

The substrate specificity varies among different enzymes, where some have active sites that can bind a broad range of different substrates, while others can only fit one specific molecule and where even the stereochemistry of the substrate can have a decisive impact. An important feature of the active site is that the product has to be able to leave and should therefore not be strongly bound. This might be a fine balance as the chemical differences between the substrates, intermediates and products can be small.

Secondly, the ability of enzymes to achieve a certain catalytic power is an intriguing issue. Several ways of acting as catalysts can be applied by an enzyme in order to lower the activation energy of the chemical reaction. Reaction rates increased by enzymes can range from 10^8 to 10^{19} relative the uncatalysed, spontaneous reactions. It is of central importance that the enzyme places the susceptible atoms of the substrates in close proximity to the catalytic groups in the active site. But proximity alone is insufficient. The reacting groups must also be in a favourable orientation for the chemistry to occur. Alignment of the relevant orbitals to overlap increases the probability of the reaction to take place.

However, not only changes in the enzyme can occur upon formation of the enzyme-substrate complex, the substrate molecule can also be strained and bonds can be distorted in order to better fit the active site. Many enzymes have active sites

designed to lower the activation energy by stabilising the transition state, thus favouring the conversion of substrate to intermediate or product.

Many enzymes utilize the formation of covalent intermediates in order to take an alternative reaction path from the uncatalysed reaction with a lower transition state energy. Amino acid residues like serine, cysteine and histidine can form nucleophilic groups that are good electron donors and form unstable intermediates that readily react further and rapidly break down to release the product.

General acid-base catalysis is due to proton donors and proton acceptors, which donates or removes protons to (or from) the reacting molecules in a concerted and/or stepwise way. An interesting feature of enzymes is that they can provide proton donor and proton acceptor groups simultaneously in a well defined orientation, a property that is impossible in solution. In this way an acidic group in one side of the active site can donate a proton simultaneously as a basic group removes a second proton in another part of the active site.

To understand how enzymes work their structures have to be considered. It has long been clear that the functional properties of proteins depend upon their three-dimensional structures. Experimentally determined three-dimensional structures by X-ray crystallography have in combination with biochemical data shown to be very powerful when characterizing enzymes and their catalytic mechanisms. A shortcoming of X-ray crystallography is that a crystal structure often only represents one state of an otherwise dynamic and varying protein structure. A new dimension of the method has therefore evolved where intermediate states during enzymatic reactions started in the crystals are trapped by freezing, followed by determination of the structure. These so-called "freeze-trapping" experiments have shown to be very useful in delineating enzymatic mechanisms and discriminating between different reaction pathways as specific intermediates can be observed.

1.2 AIM OF THESIS

To understand the enormous catalytic rate enhancement achieved by many enzymes is a major goal of many enzymologists. This thesis addresses the above discussed features for the two enzymes of the oxalate degradation pathway in *Oxalobacter formigenes*, oxalyl-CoA decarboxylase (OXC) and formyl-CoA transferase (FRC). These are two examples of enzymes that utilize the formation of covalent intermediates during catalysis. Less common intermediates are in both cases formed, where one involves a coenzyme and the other an aspartic acid residue in the active site.

OXC belongs to the family of enzymes utilising thiamin diphosphate (ThDP-the active form of vitamin B₁) for catalysis. ThDP-dependent enzymes are involved in many different pathways and catalyse a broad range of reactions. The enzyme class is known to gain a significant fraction of the catalytic power from an "entropic factor" by imposing the catalytically relevant conformation of the coenzyme and aligning the substrate in a suitable orientation for the reaction to occur. By studying a representative enzyme from the family, a lot can be learned about the catalytic mechanism of this enzyme class. The initial aim of this thesis was to determine the

crystal structure of OXC. Further, the kinetic properties of the decarboxylation reaction in OXC have been characterised and reaction intermediates have been investigated using X-ray crystallography.

FRC is a member of the recently identified Class III CoA-transferase family. As the first structure determined of this enzyme group, FRC revealed a peculiar new fold that later showed to be common to the members of the Class III CoA-transferases. The dimeric structure of these enzymes is organised like a chain, with the two monomers folded into rings interlocking each other. With a new fold and a novel set of active site residues the mechanism of Class III CoA-transferases remained to be explored. This thesis describes how the catalytic steps of FRC have been visualized through crystallographic freeze-trapping experiments, leading to elucidation and proposal of a catalytic mechanism that has been verified by several complementary biochemical methods. An intriguing question in this study has been how the enzyme protects the reactive intermediates to prevent undesired side reactions.

As further benefit this thesis will also provide information regarding the enzymes important in human oxalate homeostasis, for which the host *O. formigenes* has shown to play an important role. About 10% of all people in western countries have at some point in their lives problems with kidney stones and two thirds of all kidney stones are formed by calcium oxalate.

1.3 OXALATE HOMEOSTASIS

1.3.1 Oxalate

Oxalic acid is one of nature's most highly oxidised organic compounds. This characteristic and its ability to strongly chelate cations, especially Ca^{2+} , makes oxalate highly toxic to many life forms and complicates its catabolism and role as energy source (1). Oxalate is introduced into the human body through the diet, but also as a by-product of normal cellular metabolism (2). In humans, an accumulation of oxalate (hyperoxaluria) can in extreme cases have lethal effects, and in lower amounts cause several severe disorders, including the formation of calcium oxalate stones in the kidney (urolithiasis), renal failure, cardiomyopathy and cardiac conductance disorders (1, 3, 4). Mammals are not able to degrade oxalate and must eliminate it by excretion in the urine or through the intestine (5). The symbiotic gut-dwelling bacterium *O. formigenes* has shown to take an important role in regulating oxalate homeostasis in humans (6).

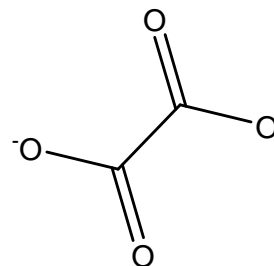


Figure 1. Oxalate

1.3.2 *Oxalobacter formigenes*

O. formigenes is a gram-negative obligate anaerobe bacterium found in the gastrointestinal tracts of vertebrates, including humans. The bacterium depends on oxalate as its sole source of energy and carbon and degrades it in a two enzyme pathway, producing formate and carbon dioxide (7). Oxalate is taken up by the bacterium through a membrane antiporter, which at the same time transports formate out of the cell. *O. formigenes* not only degrades free oxalate entering the intestinal lumen, but also creates a transepithelial gradient, favouring oxalate secretion and preventing absorption of oxalic acid in the lower tract of the intestine (8).

A direct correlation between the number of recurrent kidney stone episodes and the lack of *O. formigenes* in the intestinal flora has been demonstrated (9). A possible treatment of oxalate related diseases would be to re-colonize the gastrointestinal tract with *O. formigenes*, but de-colonized patients have not naturally regained the bacteria over several years of observation and animal experiments on rats show re-colonization to be difficult (10). In order to overcome this problem, an oxalate-degrading enzyme replacement therapy, where the two oxalate degrading enzymes are introduced into the gastrointestinal tract, has been suggested (9). *O. formigenes* central role in the human oxalate homeostasis makes the bacterium an important tool in the effort of developing new strategies for treating oxalate-related diseases (11, 12) and therapeutic studies involving *O. formigenes* are already initiated (<http://www.oxthera.com/>).

1.3.3 Oxalate catabolism

Catabolism of oxalate in *O. formigenes* is initiated by transport of the substrate into the cell. This process is mediated by the oxalate:formate antiporter, OxIT, which simultaneously discards formate into the periplasm (13). OxIT is a highly efficient transporter, and with a turnover of 1000 molecules per second and a substrate dissociation constant of 20 μM , oxalate is imported at a rate near the diffusion controlled limit (14). The three-dimensional structure of OxIT has been determined to 3.4 Å, and consists of 12 trans-membrane helices in a pseudo-twofold arrangement (15, 16).

The first step of the catabolic cycle in the cytoplasm of *O. formigenes* (Figure 2) is catalyzed by FRC. FRC catalyses the activation of oxalate by transferring a CoA moiety between formyl-CoA and oxalate, producing oxalyl-CoA and formate. OXC, as the second enzyme of the pathway, decarboxylates oxalyl-CoA and releases carbon dioxide and regenerates formyl-CoA (17, 18). The metabolic importance of these two enzymes is obvious from the observation that they together make up as much as 20% of the whole protein content of the bacterial cell (19).

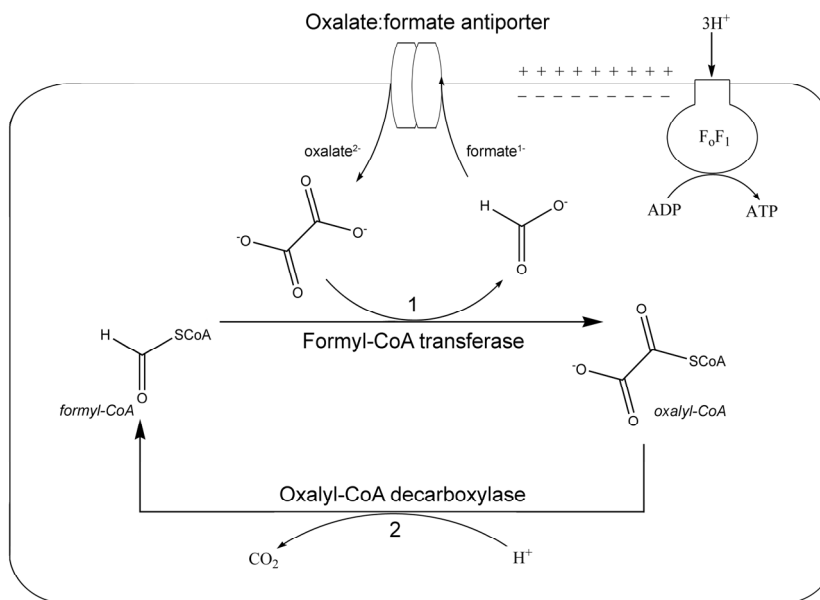


Figure 2. Oxalate catabolism and energy conservation in *O. formigenes*

Energy from the oxalate catabolism is conserved through a proton gradient which drives the ATPase in *O. formigenes*. The heterologous oxalate:formate antiporter is an electrogenic reaction in which net negative charge moves in parallel with oxalate into the cell, generating a membrane potential (13). Together with OXC, which reaction has a net stoichiometry of one proton consumed per oxalate molecule turned over, the antiporter works as an indirect ion-motive pump driving the ATP synthesis in *O. formigenes* (Figure 2).

About 99% of the oxalate in *O. formigenes* is estimated to undergo the catabolic pathway described above. The remaining 1 % is used for carbon assimilation after reduction to 3-phosphoglycerate through the glycerate pathway (20).

2 OXALYL-COA DECARBOXYLASE

A THIAMIN DIPHOSPHATE DEPENDENT ENZYME

2.1 THIAMIN HISTORY

Thiamin(e) also known as vitamin B₁, is known to play a fundamental role in energy metabolism as a major factor in the metabolism of glucose. The deficiency of thiamin usually causes weight loss, cardiac abnormalities, and neuromuscular disorders and the classical thiamin deficiency syndrome in humans goes under the name "beriberi" (21). Beriberi, which was one of the first identified nutritional deficiency diseases, has been known since antiquity, and can be found in documents as early as 808. Thiamin deficiency was, and still is to some degree, common in countries dependent on rice as primary food, and the mortality of beriberi in the beginning of the 20th century was as high as 30% in Japan. Today beriberi mainly exists in Southeast Asia where polished rice is the main sustenance and thiamin enrichment programs are not fully in place (21).

The history of thiamin begins with beriberi. After a physician in the Japanese Navy in the 1880s realized and pointed out the correlation between the polished rice diet of the sailors and the disease, a new diet was implemented containing more vegetables, fish and meat, and the incident of the disease in the Japanese Navy dropped from 40% to 0% in six years. It was soon discovered that even fowls fed on a pure polished rice diet developed this disease and gradually it became evident that the polished rice caused beriberi while the rice hull prevented and even cured the disease (21). An "anti-beriberi" factor was isolated from rice polishing and named 'Vitamin' for vital amine, and in 1926 it was crystallised and soon the structure of this new compound then called aneurin (for antineuritic vitamin) was reported. Unfortunately, the first structure missed the sulfur atom, but the correct structure together with the synthesis was published in 1936. The American Medical Association, which did not accept the names under which the compound was known (anti-beriberi factor, antineuritic vitamin, vitamin B, vitamin B₁), asked for a new name and so the name thiamin was invented, reflecting the vitamin's amine nature and content of sulfur (22).

2.2 THIAMIN DIPHOSPHATE

Vitamins commonly play the role as building blocks of coenzymes, organic molecules that facilitate the chemical reactions catalysed by enzymes. The major biologically active form of thiamin is thiamin diphosphate (ThDP), also known under the names thiamin pyrophosphate and cocarboxylase. ThDP is utilized by enzymes that perform a wide range of catalytic functions. It is an essential coenzyme in biocatalysis and mediates important reactions in carbon metabolism, including the oxidative and non-oxidative decarboxylation of α -keto acids, ketol transfer between sugars, formation of amino acid precursors and electron transfer reactions. During almost 70 years of extensive solution and crystallographic studies,

ThDP has shown to be a peculiar cofactor that with support of the enzyme performs most of the catalysis by itself (Reviewed in 23, 24).

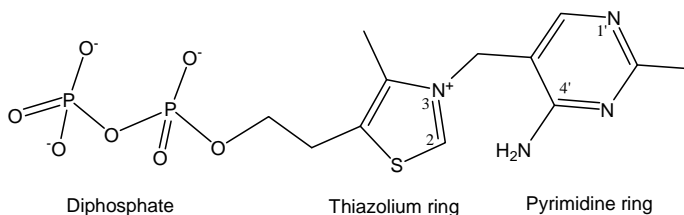


Figure 3. Thiamin diphosphate

2.2.1 The coenzyme

Thiamin diphosphate is comprised of three groups, a central catalytic thiazolium ring flanked on one side by a 4'-aminopyrimidine ring (the thiamin core) and on the other end by a diphosphate group. Initially, the aminopyrimidine ring was believed to be the catalytic group of the cofactor but it was soon shown that the C2 position of the thiazolium ring is where the reaction takes place, and where deprotonation initiates the catalytic cycle (25). The thiazolium ring acts as an electron sink during the formation of this ylid, partly by stabilising it with the adjacent positive charge of the quaternary ammonium but also by the ability of the d-orbitals of sulfur to accept some of the negative charge. However, both ring moieties of the coenzyme contribute during catalysis, and the 4'-aminopyrimidine ring likely participates in the reaction as an intramolecular general acid-base catalyst via the rare 1',4'-iminopyrimidine tautomer (23, 25-27) .

It has been shown by $^2\text{H}/^1\text{H}$ exchange that the C2-proton dissociation rate for free ThDP is too slow to fit the demand of the active enzymes (25, 28). In order for the ThDP-dependent enzymes to achieve the measured catalytic power, the dissociation rate has to be increased at least 4 orders of magnitude by the interactions with the enzyme. This is one of the main contributions by the thiamine diphosphate dependent enzymes to their catalytic rate enhancements.

2.3 THIAMIN DIPHOSPHATE DEPENDENT ENZYMES

The first three-dimensional structure of a ThDP-dependent enzyme determined was of transketolase (TK) in 1992 (29). Soon crystal structures of pyruvate oxidase (POX) (30) and pyruvate decarboxylase (PDC) (31) followed, and at the time of writing there are over 18 ThDP-dependent enzymes of known structure, with many of them determined from different species as well. Only ThDP-dependent enzymes of known three-dimensional structure will be discussed in the following section. A summary of all structures in the Protein Data Bank, including primary structure references, is found in Table 1.

Table 1. Members of known three-dimensional structure in the five families of ThDP-dependent enzymes

Abbreviation	Enzyme name	Structure references
POX or "decarboxylase" family-		
POX	Pyruvate oxidase	(30)
PDC	Pyruvate decarboxylase	(31, 32)
IPDC	Indolepyruvate decarboxylase	(33)
BFD	Benzoylformate decarboxylase	(34)
OXC	Oxalyl-CoA decarboxylase	(35)
AHAS	Acetohydroxyacid synthase	(36)
ALS	Acetolactate synthase	(37)
BAL	Benzaldehyde aldolase	(38)
CEAS	N ² -(2-carboxyethyl)arginine synthase	(39)
PPDC	Phenylpyruvate decarboxylase	(40)
KdcA	Branched chain α -keto acid decarboxylase	(41)
TK family		
TK	Transketolase	(29)
DXS	1-deoxy-D-xylulose-5-phosphate synthase	(42)
OR family		
PFOR	Pyruvate:ferredoxin oxidoreductase	(43)
2-ketoacid dehydrogenases - one chain		
PDH-E1	E1 of Pyruvate dehydrogenase complex gram-negative bacteria and actinomycetes	(44)
2-ketoacid dehydrogenases - two chains		
PDH-E1	E1 of Pyruvate dehydrogenase complex eukaryotes and gram-positive bacteria	(45)
OGDH-E1	E1 of 2-ketoglutarate dehydrogenase eukaryotes and gram-positive bacteria	(46)
BCKD-E1b	E1 of Branched-chain 2-ketoacid dehydrogenase, eukaryotes and bacteria	(47-50)

2.3.1 The five subfamilies

ThDP-dependent enzymes can be divided into five subfamilies based on their three-dimensional structures and sequence analysis. The largest group, named the POX family after the first structure determined in the group, includes a large fraction of the ThDP-dependent enzymes with determined structure, including OXC. Some of the most studied members are PDC, benzoylformate decarboxylase (BFD), acetohydroxyacid synthase (AHAS), acetolactate synthase (ALS) and benzaldehyde aldolase (BAL). The reaction catalyzed (or part of it) by most of the enzymes is the decarboxylation of a 2-ketoacid, and among all the members, POX stands out as the only enzyme of the group catalyzing a redox reaction.

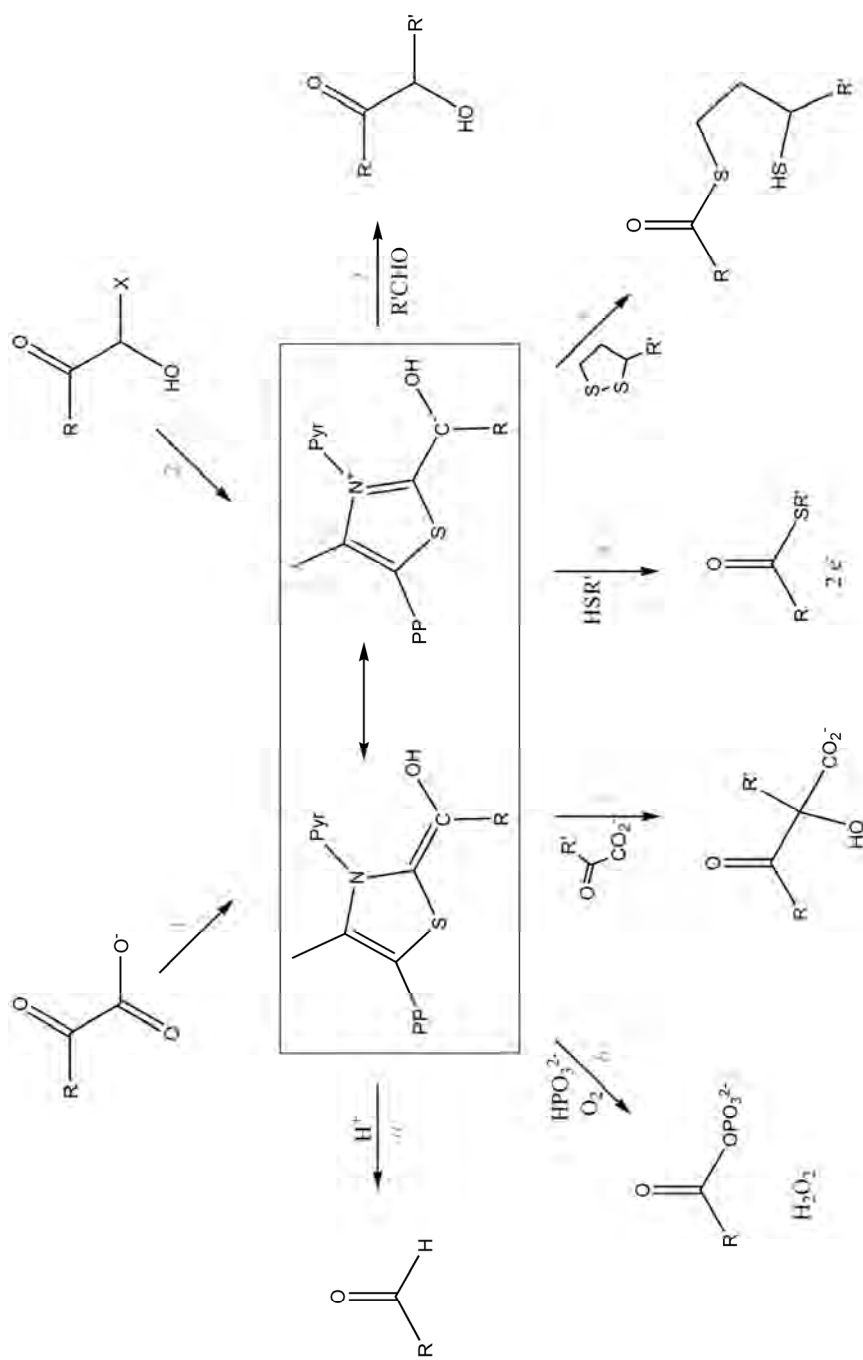


Figure 4. A summary of reactions catalysed by ThDP-dependent enzymes. Either a 2-ketoacid (upper left) or an acylloin (upper right) substrate is cleaved adjacent to the carbonyl group forming the covalent complex between the remainder of the substrate and ThDP. The formed enamine/α-carbanion intermediate (enclosed in the central box) then reacts with the acceptor substrates in one of the routes *a-f*, completing the catalytic cycle and releasing the product. This representation of the reactions is adapted from (51).

Most of the reactions of the POX family members are summarized in Figure 4, where the substrate comes in through path 1 and is decarboxylated forming the enamine/ α -carbanion intermediate. BAL and carboxyethylarginine synthase (CEAS), as exceptions, catalyse a reaction with an acyloin substrate, entering through path 2. The fate of the intermediate then varies for the different members. The 2-ketoacid decarboxylases react with a proton (route *a*) releasing an aldehyde, while POX takes route *b* with a phosphate and oxygen as second substrates forming acetyl phosphate and hydrogen peroxide. AHAS and ALS react with a second 2-ketoacid following route *c*.

The second subfamily, the TK family, has two members of known structure TK itself and the recently determined 1-deoxy-D-xylulose-5-phosphate synthase (DXS). In addition to these two, phosphoketolase and dihydroxyacetone synthase also belong to the group (52, 53). The TK reaction is defined in Figure 4, through the incoming path 2 and then outgoing route *f*.

The next family contains only one member of known structure, pyruvate:ferredoxin oxidoreductase (PFOR) (route 1*d* in Figure 4). It is difficult to define what other enzymes belong to the family of PFOR, but there are several variants of the enzyme with different numbers of subunits and domains, dependent on the identity of the final electron acceptor (ferredoxin, flavodoxin or NADP⁺). Whether or not these variants should be defined as different enzymes or just variants of PFOR is not clear.

The final two subfamilies of ThDP-dependent enzymes are the 2-ketoacid dehydrogenases (route 1*e*), which are multienzyme complexes with three major components where E1 is the ThDP-dependent component. The 2-ketoacid dehydrogenases are divided into two families depending on whether they consist of one or two chains. Pyruvate dehydrogenases (PDHs) from gram-negative bacteria and actinomycetes stand alone in the one-chain group, while the two-chain family contains the E1 component of 2-ketoglutarate dehydrogenase and E1 of PDH from eukaryotes and gram-positive bacteria as well as the branched-chain 2-ketoacid dehydrogenases (BCKD).

2.3.2 Subunit architecture and oligomeric state

The common architecture of ThDP-dependent enzymes consists of three α/β -type domains (54). There are a few exceptions to this fold where the enzymes have evolved differently and the domain order is switched or one of the domains is missing (55). The domains are all comprised of a central β -sheet flanked by α -helices on both sides. Two of the three domains form the interactions with the cofactor and are named the pyrimidine- and pyrophosphate domains (PYR- and PP-domains), explaining which part of ThDP they bind. These two domains are topologically related, while the third so called regulatory (R-domain) has a slightly different fold. The R-domain is commonly also named domain X due to its unknown function in several of the family members. Some of the members have evolved a nucleotide binding site in this domain where FAD binds in POX and AHAS (30, 36), and ADP has been identified to bind in OXC as will be described later on in this thesis.

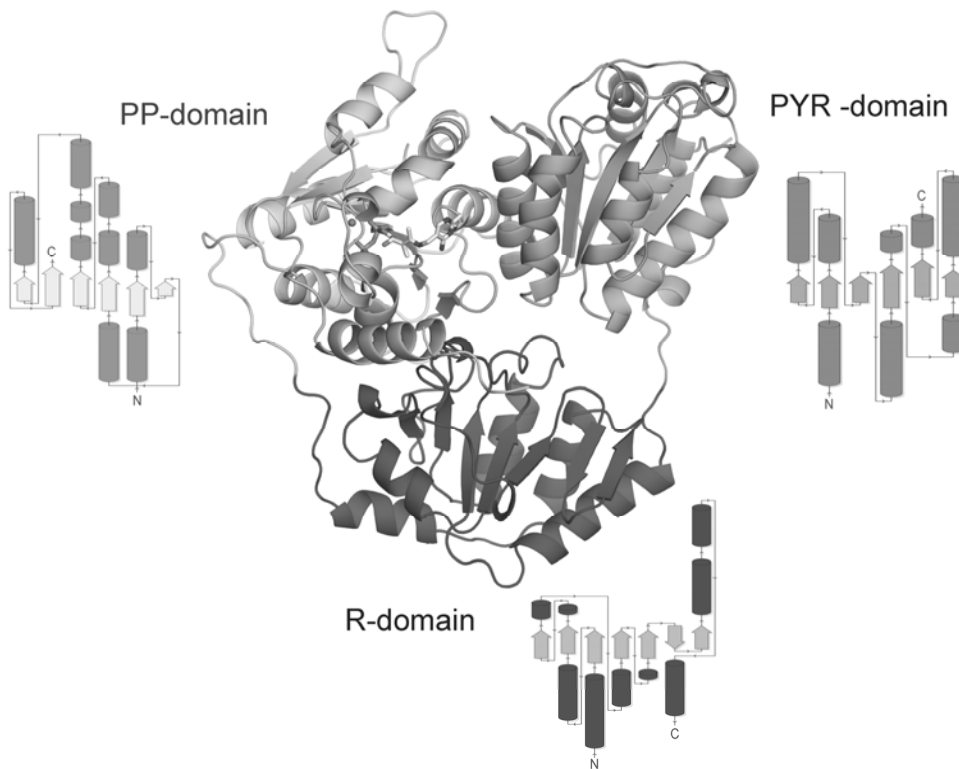


Figure 5. An example of the ThDP-dependent enzyme fold. The monomer of PDC from *Zymomonas mobilis* (1zpd) (32) and topology diagrams of the three domains. Topology diagrams are adapted from PDBsum (56).

A feature shared by several ThDP-dependent enzymes is a C-terminus which in the absence of substrate adopts a flexible structure without secondary structure elements, but that upon binding of substrate folds down into an α -helix closing over the active site. Mutational studies with AHAS, *Zm*PDC and OXC where the C-termini were truncated, have proven closure of the active site to be essential for catalysis in these enzymes (57-59). Not only does the C-terminus control the accessibility to the active site, it also protects the activated coenzyme and creates a hydrophobic environment required for decarboxylation.

The coenzyme is bound in the interface between PYR- and PP-domains from two different subunits, rendering the minimal functional unit of ThDP-dependent enzymes a dimer. In the case of TK, AHAS, ALS and KdcA the dimer represents the biological unit but most other family members consist of two dimers that form a tetramer.

2.3.3 Coenzyme binding

All ThDP-dependent enzymes require a divalent metal ion for coenzyme binding. The function of the metal ion is to attach the pyrophosphate moiety with a set of conserved amino acids of the PP-domain (GDG/SX₂₅₋₃₀NN motif) (60) and thereby

anchor ThDP to the enzyme. The ion specificities of the enzymes are normally low but no activity is seen in the absence of divalent ions.

One of the most striking findings from crystallographic studies of ThDP-dependent enzymes is the so-called “V” conformation of the coenzyme. This conformation, observed in all of ThDP-dependent enzymes of known structure, describes the position of the 4'-aminopyrimidine ring and the thiazolium ring with respect to each other (61). It is clearly not a low energy conformation and is seldom found in thiamin derivatives in the absence of enzyme (62, 63). Several features of the environment in the protein might help to stabilize the V conformation, in particular a conserved bulky hydrophobic residue (Met, Ile or Leu) positioned below the thiazolium ring (64). The N4' and C2 atoms of ThDP are placed in close proximity in the V conformation with a distance of approximately 3.0-3.6 Å between the two atoms.

Another conserved feature in the binding of ThDP is that hydrogen bonds are formed to all the nitrogen groups of the 4'-aminopyrimidine. These interactions have shown to be crucial for catalysis and play important roles during activation of ThDP.

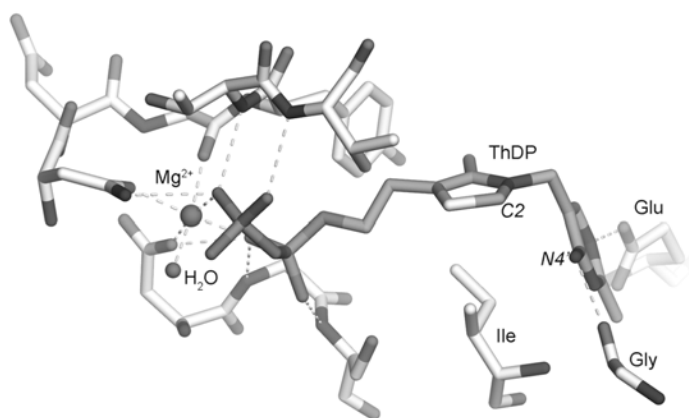


Figure 6. The conserved ThDP-binding anchored by a magnesium ion

2.3.4 Coenzyme activation

The currently well accepted mechanism of ThDP catalysis is initiated by activation of the coenzyme. The enzyme has been shown to play a decisive role during this step by a conserved glutamic acid residue (25). A strong hydrogen bond between the glutamic acid and N1' of the pyrimidine ring stabilizes the unusual 1',4'-iminopyrimidine tautomer of the coenzyme. With the geometry and basicity of the imino group, 4'-NH is ideally positioned for abstracting a proton from C2 and creates the reactive ylid (25, 65). The importance of the glutamic acid - N1' interaction has been shown by mutagenesis studies, where the hydrogen bond was disrupted and catalysis was severely impaired (66-70). A conserved glycine residue, which hydrogen bonds N4' through the main chain carbonyl, further contributes to the activation of the cofactor by optimally orienting N4' to point its lone pair at the C2 hydrogen (34).

2.4 THIAMIN DIPHOSPHATE DEPENDENT DECARBOXYLATION

The cofactor activation described in the previous section is common to all ThDP-dependent enzymes. This section, describing the following catalytic steps, will focus mainly on the subfamily of decarboxylases where OXC is included.

There is a large diversity in active site residues among the ThDP-dependent decarboxylases, and hardly any strict sequence conservation exists except for the residues that are directly involved in cofactor binding and activation. One notable exception is that many of the decarboxylases, including PDC, IPDC and KdcA, all have two conserved consecutive histidine residues positioned in the active site. Two equivalent histidines are also found in BFD, although in this case they are derived from different subunits. OXC, POX and AHAS do not contain any histidine residues or other conserved polar residues in the active site and BAL has only one histidine positioned further away in the active site. With a large diversity of active site residues, but still a very similar reaction, it is clear that different active site groups must perform the same task in the different decarboxylases. It has however been concluded that the enzymic groups mainly contribute by aligning the different substrates and many of the catalytic steps are accounted for by ThDP itself. With the exception of the glutamic acid activating ThDP, there is only one proton transfer step during the non-oxidative decarboxylation reaction that is not accounted for by the coenzyme itself. The currently accepted reaction mechanism is presented in Figure 7.

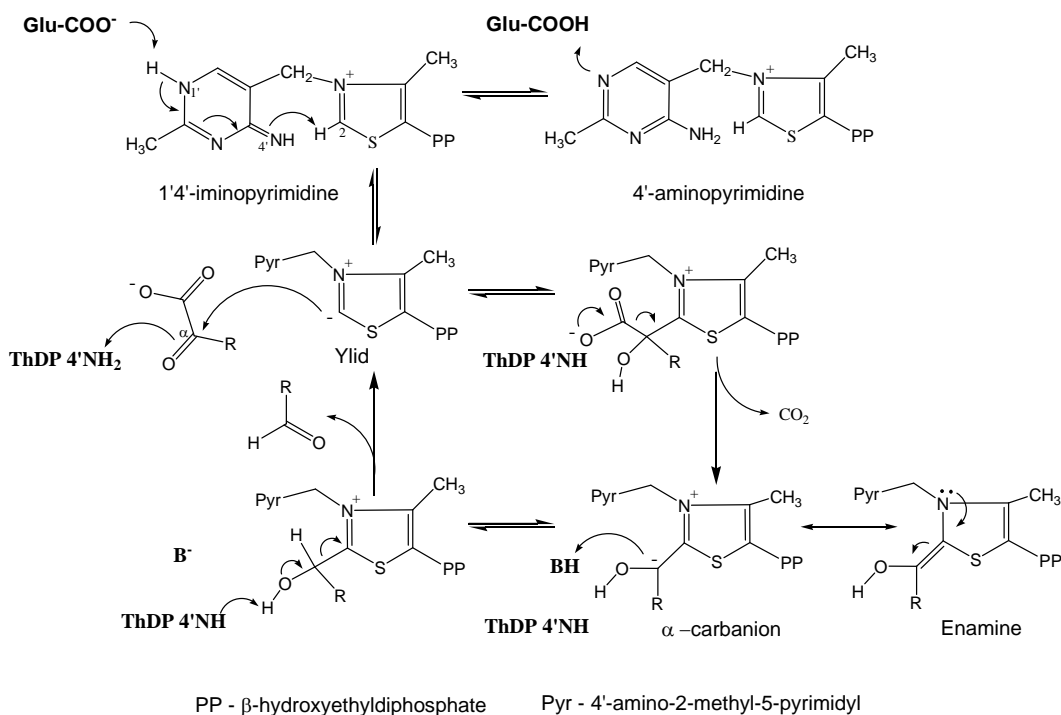


Figure 7. Non-oxidative decarboxylation by ThDP-dependent enzymes

2.4.1 Decarboxylation

After the initial step of cofactor activation, a nucleophilic attack by the coenzyme ylid at the C α atom of the substrate carbonyl results in the first covalent reaction intermediate between the coenzyme and substrate. Upon formation of the covalent bond, a developing negative charge generated at the carbonyl oxygen of the substrate has to be stabilized and is thus protonated, most probably by 4'NH₂. The decarboxylation and release of CO₂ (or for some other members RCOOH) follows rapidly, resulting in the α -carbanion/enamine intermediate.

2.4.2 The α -carbanion/enamine intermediate

The α -carbanion/enamine intermediate is of central importance in thiamin catalysis, depending on the fate of the intermediate a variety of enzymatic functions can be derived (Figure 4). The nature of the α -carbanion/enamine intermediate has long been debated in ThDP chemistry- whether the intermediate has a dominant non-planar α -carbanion character or mostly ensembles the stabilized planar enamine is not known. For the large group of non-oxidative decarboxylases where protonation of the α -carbanion is the following step, relaxation in the enamine would impede the reaction and recent studies show that these enzymes might keep the intermediate in the most reactive resonance form with predominant α -carbanion character (71). For other ThDP-dependent enzymes, where an acceptor substrate is to be attached to C α , protonation is an adverse side reaction and it is suggested that the intermediate is stabilized with predominant enamine character until binding of the second substrate.

2.4.3 Product formation and release

After protonation or attachment of the acceptor substrate to C α follows C2-C α bond cleavage and product release. The C α -OH is deprotonated during this step and the ylid is regenerated completing the catalytic cycle.

The identity of the group acting as proton donor to the α -carbanion/enamine is ambiguous in the ThDP-dependent non-oxidative decarboxylases, due to the diversity in surrounding functional groups. A histidine residue has been proposed to perform this task in BFD (72), but the corresponding residue in PDC has been shown to be involved only in the steps up to and including decarboxylation (73). The proton source is clearly not conserved between the different members, and none of the members has the donor identity settled even though many possibilities have been proposed.

2.5 RESULTS ON OXALYL-COA DECARBOXYLASE

Structural studies of OXC were long hampered by irreproducibility of crystals and low diffraction quality. The first break-through came when a crystal produced from seleno-methionine substituted protein showed diffraction to nearly 4 Å resolution.

Further crystallisation trials and change of protein storage buffer resulted in a new crystal form. Among several crystals tested one showed diffraction to 1.7 Å resolution and data was collected. The later finding that the crystal was highly merohedrally twinned did not hamper structure solution and the complete structure of OXC could be determined. The new crystal form later showed to be useful for freeze-trapping experiments and the complete reaction could be structurally visualised after solving more than 40 different complex structures. The structural work has been complemented with kinetic characterisation of the wild type enzyme as well as mutant variants.

2.5.1 Crystallisation and structure determination (Paper I)

Recombinant OXC produced in *Escherichia coli* and purified to homogeneity was used for crystallisation by the vapour diffusion method. Seleno-methionine substituted protein in the phosphate elution buffer from the purification was crystallised at a concentration of 2.5 mg/mL resulting in 0.1 x 0.1 x 0.2 mm crystals within 48h. The best data obtained to a resolution of 4.1 Å was collected from a crystal belonging to the space group P4₂2₁2 with one monomer in the asymmetric unit. The low quality of the data impeded determination of the phases using the anomalous data and the molecular replacement approach was therefore applied using the closest homologue, AHAS (23 % sequence identity) (36), as search model. The incomplete structure determined had only partial sequence assignment and building and refinement was never completed as higher quality data was obtained.

OXC was dialysed into a new buffer devoid of phosphate and 10 mM ThDP, 10 mM MgCl₂ and 1 mM CoA was added before screening for new crystallisation conditions was performed. Optimised crystals of a new morphology were obtained with a precipitant solution containing PEG 550 monomethyl ether and CaCl₂. Data was collected to 1.73 Å resolution from a crystal that from the intensity statistics showed to be hemihedrally twinned. With a two-fold twin operator along c, a*, b* and a twin fraction of 0.44, the data in the true space group P3₁21 mimicked 622 symmetry. Full details of the characterisation of twinning and determination of the true space group are described in Paper I. The previously solved incomplete low resolution structure was used as search model for obtaining the phases by molecular replacement. Two monomers were placed in the asymmetric unit of the true space group. Inspection of the crystal packing revealed the non-crystallographic two-fold axis to be parallel to the twin axis, a feature known to promote twinning. Manual model building and refinement using the twin protocols in CNS (74) resulted in a structure including the amino acid residues 7-552 out of 568.

2.5.2 Structure of the holoenzyme (Paper II)

Paper II of this thesis includes the characterisation of the OXC holo structure. The 61 kDa subunit of OXC has the conserved three-domain fold common among

ThDP-dependent enzymes. The monomers assemble into homotetramers, which were observed in the crystals where two dimers in adjacent asymmetric units generate the tetramer by a crystallographic 2-fold axis. The oligomeric form was verified by size-exclusion chromatography as well.

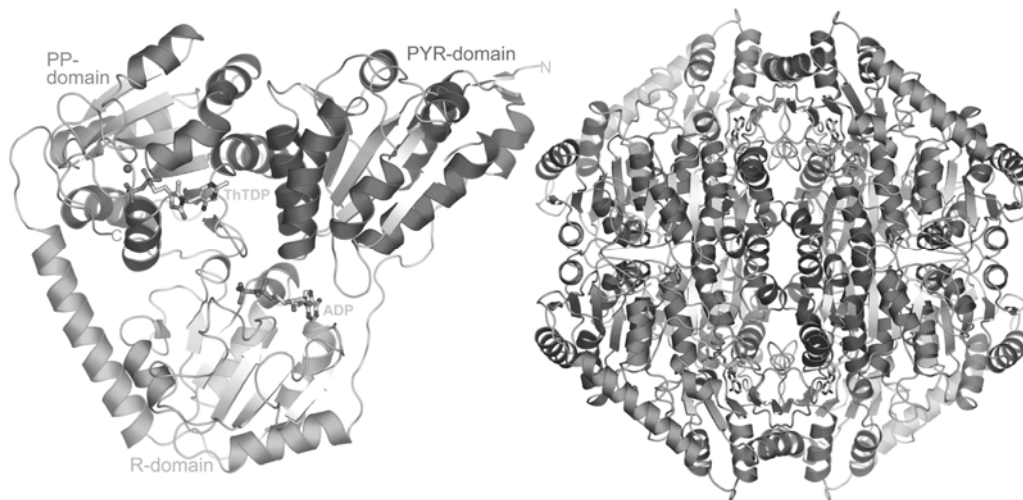


Figure 8. The OXC monomer and homotetramer shown in cartoon representation. ThTDP and ADP are displayed as stick models

2.5.2.1 Active site

The interactions with and conformation of the bound coenzyme are strictly conserved between ThDP-dependent enzymes, including OXC, and it is clear from the conserved fold that they derive from a common ancestor despite the lack of overall sequence conservation. Interestingly, OXC does not share any of the active site residues not involved in co-factor binding with any of the other decarboxylases and a unique set of active site residues was identified for OXC (Figure 9), from which a plausible reaction mechanism was suggested. The thiazolone derivative of ThDP was observed in the OXC active site, probably as a result of exposure by intense X-rays.

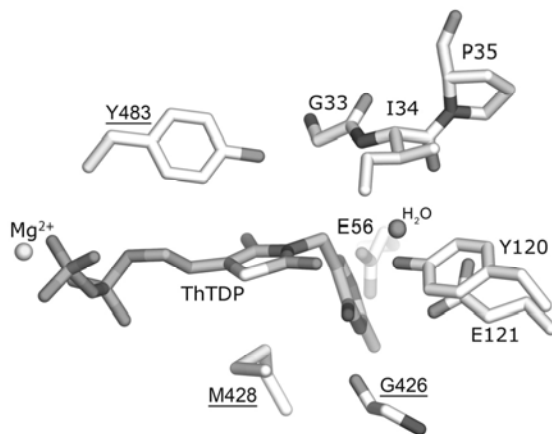


Figure 9. 2-thiazolone-ThDP bound in the OXC active site. Underlined labels represent residues from the adjacent subunit.

2.5.2.2 Activation by ADP

After completing the structure of OXC, two large blobs of electron density remained in the R-domain at the location corresponding to where FAD binds in AHAS (36). CoA, which was included in the crystallisation condition, was initially modelled into the density but it was soon clear that the 5'-phosphate attached to the ribose moiety could not be fit into the binding site without major movements of surrounding residues. The lack of electron density for the pantetheine tail also contributed to the conclusion that the density resulted from an ADP molecule, which was successfully refined into the structure (Figure 10). Kinetic measurements proved ADP to have a stimulating effect on the enzyme by increasing the specific activity already at micromolar concentrations, while ATP had no effect (Figure 10). The importance of oxalate degradation for ATP generation supports the finding that ADP is a high affinity activator of OXC, which most probably is of physiological relevance in *O. formigenes*.

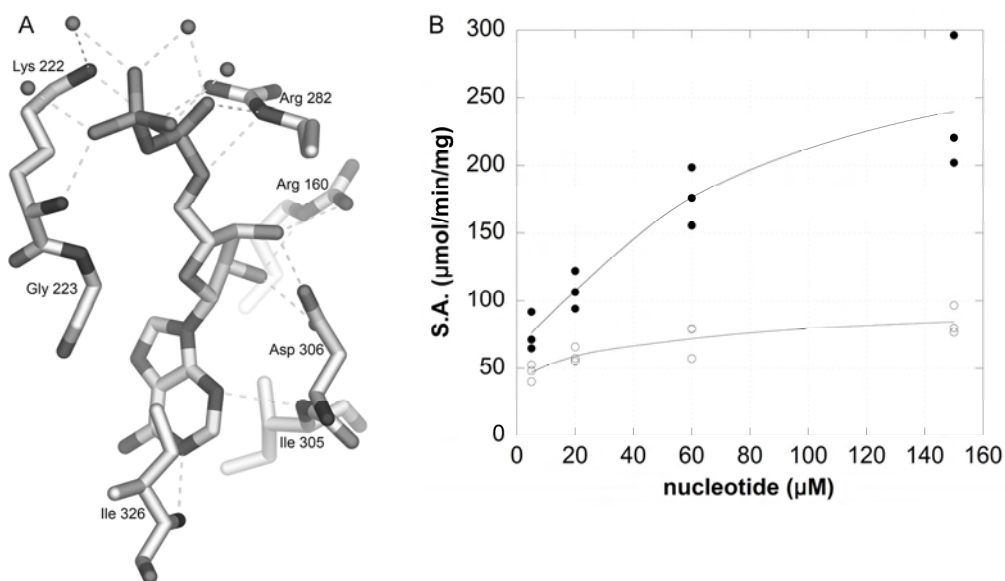


Figure 10. **A)** Interactions between ADP and the R-domain of OXC. **B)** ADP activation of OXC. The enzyme was assayed with 500 μM oxalyl-CoA in the presence of ADP (filled circles) or ATP (open circles)

2.5.3 Crystallographic snapshots (Paper III)

2.5.3.1 Substrate complex with 3'-deazaThDP

OXC stands out among its homologues by accepting a much larger substrate than many of the other enzymes in the family, and the substrate binding site remained to be elucidated after the discovery that the nucleotide binding site in the R-domain was occupied by ADP in OXC. The binding site of oxalyl-CoA was identified by replacing ThDP with the inhibitor 3'-deazaThDP (dzThDP), crystallise the complex

and then soak oxalyl-CoA into the crystals. dzThDP has shown to be an extremely efficient inhibitor of many ThDP-dependent enzymes (75, 76). The lack of a positive charge in the thiazolium ring by replacement of N3 by a carbon atom prevents activation of the cofactor and formation of the ylid, and no attack on the substrate can take place (Figure 11). With an overall uncharged thiazolium ring dzThDP mimics the charge state of the ylid and many enzymes have been shown to bind the inhibitor even more strongly than the actual coenzyme (76). Dialysis against EDTA at an elevated pH was performed in order to generate the apoenzyme by removing the Mg-ion and thereby ThDP anchored by it.

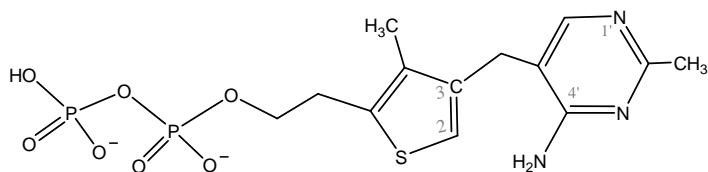


Figure 11. 3'-deazaThDP

The substrate binding site in OXC is positioned in a cleft between the R- and PP-domain. Most of the interaction between the protein and the CoA carrier can be accounted for by three arginine residues that position the diphosphate by several hydrogen bonds. The pantetheine tail reaching into the active site forms no direct interactions with the protein but is surrounded by structurally ordered water molecules. The active site residues Ser-555, Tyr-483, Ile-34, Tyr-120 and Glu-121 all contribute towards positioning the oxalate moiety in an orientation favourable for reaction, with a distance of approximately 3 Å between the alpha-carbon and C2 of ThDP (Figure 12).

2.5.3.2 C-terminal lid

In the holo structure of OXC the electron density for the C-terminus abruptly ends at residue 552 and the orientation of the remaining 16 residues could not be detected. Upon substrate binding the residues 553-565 organise and fold into a lid covering the active site. A truncation mutant lacking the C-terminus showed no activity, proving the essentiality of these residues for aligning the substrate and providing a hydrophobic environment facilitating decarboxylation.

Two reference structures of OXC were determined in order to localize what triggered the C terminal organisation. The structure of OXC with dzThDP still had an unordered terminus so the charge state of the cofactor was clearly not the triggering factor as earlier was suggested in a study of PDH-E1 (76). The second structure analysed was of holo OXC in complex with CoA. The C-termini were folded in this complex, leading to the conclusion that binding of the CoA carrier is what triggers closure of the active site.

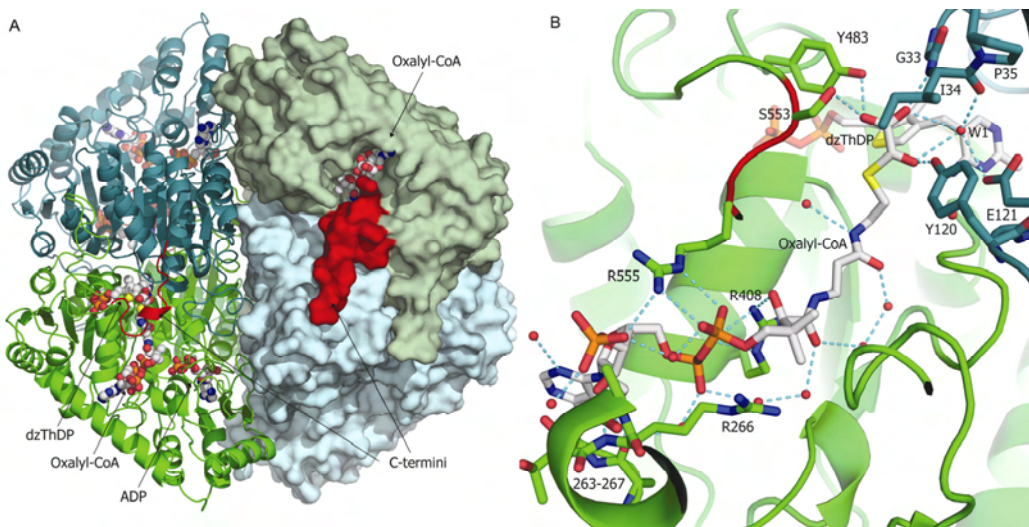


Figure 12. **A)** The OXC tetramer with one of the catalytic dimers displayed in surface mode. dzThDP, Oxalyl-CoA and ADP are shown as sphere models and the C termini that organises upon substrate binding are shown in red. **B)** A closer view of the substrate binding in OXC. For clarity, the C-terminal residues 556-565 have been omitted in the picture. Hydrogen bonds are displayed as dashed lines.

2.5.3.3 The non-planar covalent reaction intermediate

Freeze-trapping experiments performed on crystals of holo OXC soaked with oxalyl-CoA resulted in several intermediate structures along the reaction. All experiments were performed at 277 K in order to slow down the reaction. Soaking times shorter than 8 minutes resulted in low occupancy of reactants and soaks for more than 10 minutes resulted in heterogeneous complexes where some molecules had turned over to product. No pre-decarboxylation covalent complexes could be observed showing that the decarboxylation step is very fast and occurs almost simultaneously as the cofactor attacks the substrate. The post-decarboxylation intermediate complex presented in paper III was best modelled with a non-planar C α atom oriented slightly out of the thiazolium plane, with a close interaction between the substrate carbonyl oxygen and N4' of ThDP. The same features have previously also been observed for human BCKD-E1b (77).

As described in the introduction, there is one proton transfer step during ThDP decarboxylation that is not accounted for by the coenzyme. The crystal structures of OXC show that none of the active site residues are close enough to perform this protonation of the α -carbanion (BH in Figure 7). Mutational studies of the surrounding residues further confirmed that none of the residues are absolutely crucial for the reaction to occur, which substantiate a hypothesis that the proton must be donated from elsewhere. In the freeze-trapped post-decarboxylation

reaction intermediate structure there are two water molecules organised above the covalent complex. One of these molecules is perfectly positioned for donating a proton to the intermediate complex. Bond distances and the intermediate conformation indicate that the proton transfer has taken place and that the covalent complex between ThDP and the product is the species trapped in the crystal.

2.5.4 Concluding remarks on oxalyl-CoA decarboxylase

The three-dimensional structure of OXC was after extensive crystallisation trials determined at high resolution. The existence of merohedral twinning necessitated thorough analysis of the data, but the structure could be determined and refined by the use of established crystallography software.

The holoenzyme structure led to the discovery that ADP acts as a high affinity activator of OXC, which was followed up and established through kinetic measurements. Further crystallographic data revealed the substrate binding site and structural proof for closure of the active site upon substrate binding was provided.

Freeze-trapping experiments identified a covalent reaction intermediate in OXC. The non-planarity of the intermediate led to the interpretation that the species observed was the product covalently bound to C2 of ThDP. A structurally organised water molecule above the intermediate, together with mutagenesis data showing that none of the active site residues were absolutely crucial for activity (except the cofactor activating glutamate), led to the conclusion that the proton in the final protonation step in OXC is provided by a water molecule.

Several crystal structures of other non-oxidative ThDP-dependent decarboxylases also display structurally ordered water molecules in the active sites. It can be speculated that these also might be utilised to derive the proton for the α -carbanion. However, further structural and biochemical studies will have to be implemented in order to settle the origin of the proton in the other members.

3 FORMYL-COA TRANSFERASE

A CLASS III COENZYME A TRANSFERASE

3.1 THE THIOESTER BOND AND COENZYME A

In an abiotic world, phosphate was scarce and other kinds of molecules than the present specialized energy source ATP must have served as energy-rich compounds. One candidate for a primitive "high-energy" compound is the thioester. The thioester bond is higher in energy than the normal ester bond due to the large radius of sulfur, which leads to less resonance stabilisation, with less overlap of the π -electrons between the carbon and sulfur atoms compared to between the carbon and oxygen atoms in an ester (78). In modern metabolic pathways the thioester bond appears in reaction intermediates (involving cysteins in enzymes) and in acyl derivatives of CoA including acetyl-CoA, the common product of carbohydrate, fatty acid and amino acid catabolism entering the citric acid cycle. The thioester bond in acetyl-CoA has a free energy of hydrolysis of $-31.5 \text{ kJ}\cdot\text{mol}^{-1}$, which is slightly more exergonic than the hydrolysis of ATP.

CoA functions as the most prominent carrier of acetyl and other acyl groups in all living systems ("A" in CoA stands for "acetylation"). It was discovered in 1945 by Lipmann, who identified it as a heat-stable cofactor required for certain biological acetylations (79). Today CoA is known to be involved in various essential pathways, including the synthesis of fat, cholesterol and steroid hormones, the neurotransmitter acetylcholine and the hormone melatonin. Heme also requires CoA containing components for its synthesis and metabolism of a number of drugs and toxins by the liver requires CoA (80). In total CoA is estimated to be utilized by as many as 4% of all enzymes (81). Unlike most cofactors that remain bound to a single enzyme, CoA predominantly acts as a diffuse carrier of acyl groups from one enzyme-catalysed reaction to another.

CoA is derived from pantothenic acid, a member of the vitamin B family. Naturally occurring pantothenic acid deficiency in humans is rare, as the vitamin is readily accessible in diverse dietary sources, and has only been observed in cases of severe malnutrition. No particular disease has been linked to the deficiency of pantothenic acid (82).

3.1.1 Structure of coenzyme A

The covalent structure of CoA shown in Figure 13 was elucidated in 1953 (83). CoA consists of a pantetheine arm, containing a pantothenate and β -mercaptoethylamine group, which is attached to a 3' phosphorylated ADP moiety. Although the structure of CoA is complex, it is functionally a simple molecule. The acyl group is attached to the sulfhydryl group at the end of the pantetheine and the reactions of CoA thioesters only involve the thioester bond and/or the acyl group. The rest of the CoA molecule serves as a recognition element for binding by enzymes.

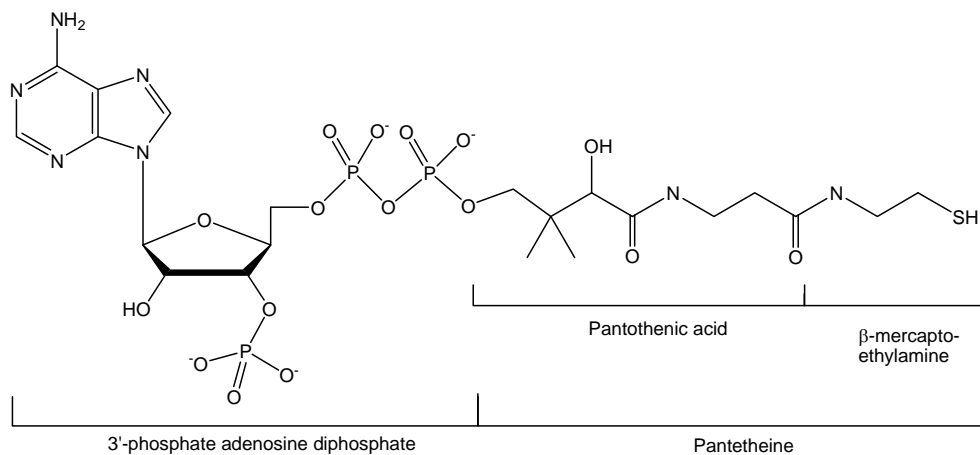


Figure 13. Schematic drawing of CoA

The fairly complex structure of CoA is mirrored in the large variety of conformations it has been shown to adopt upon binding to proteins. The adenosine moiety mostly shows the same conformation with a 2'-endo conformation in the majority of the structures, and the pantetheine arm is in most cases extended. The large diversity is therefore mostly due to different extents of bending at the pyrophosphate group, and the pantetheine arm can be found in conformations almost parallel to the adenosine or pointing in the totally opposite direction (84).

3.1.2 Binding of coenzyme A in proteins

ADP is a common building block of many cofactors, and in addition to CoA, it is also included in NAD(P), FAD and ATP among others. A conserved binding mode to proteins has been concluded for NAD(P) and FAD where adenosine binds to a Rossmann fold (85) with the pyrophosphate hydrogen bonded to the main chain NH group at the N-terminus of the α -helix of the $\beta\alpha\beta$ fold. Other conserved ways of binding proteins have been identified for ATP, where the P-loop is the most common motif (86). In contrast, the structures of CoA binding proteins show a high diversity in folds, among others, CoA has been found bound to TIM barrels, helical bundles and also the Rossmann fold (84). Several structures of CoA binding proteins have been determined to date, but no conserved binding motif or fold has been identified for CoA.

3.2 COENZYME A TRANSFERASES

CoA-transferases catalyse the reversible transfer reactions of a CoA carrier from a donor CoA thioester to a carboxylic acid acceptor generating the free donor acid and a new acyl-CoA. CoA-transferases are involved in a broad range of biochemical processes in both bacterial and eukaryotic species, and show a diverse range of substrate specificities. Three classes of CoA transferases have been defined based on sequence and mechanistic criteria (87).

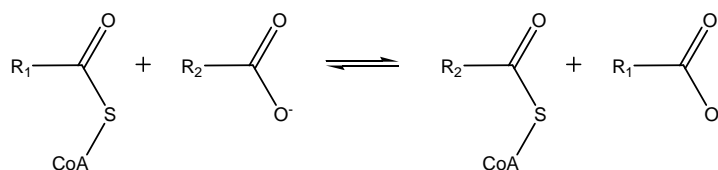


Figure 14. General CoA transfer reaction. For the forward reaction $R_1\text{COO}^-$ and $R_2\text{COO}^-$ refer to the donor and acceptor acyl groups, respectively

3.2.1 Class I

Members of the Class I CoA-transferase family catalyse the transfer of 3-oxyacids (88-90), short chain fatty acids (91-93) and glutaconate (94, 95) with the use of succinyl-CoA or acetyl-CoA as CoA donors. Most Class I enzymes consist of two subunits in different oligomeric states ($\alpha_2\beta_2$ or $\alpha_4\beta_4$) with the monomers resembling an open α/β fold. Members with homotetrameric assembly also exist, where the subdomains are orthologous to the corresponding α and β subunits of the other enzymes (93, 96). These enzymes have a well characterized reaction mechanism and operate with a classical ping-pong mechanism involving a conserved glutamic acid in the active site that acts as acceptor of covalently bound intermediates (97, 98) (Figure 15). The reaction is initiated by an attack by the glutamate residue at the donor CoA-thioester yielding an enzyme-bound acyl-glutamyl anhydride and free CoAS^- . The CoAS^- which remains bound in the active site next attacks the glutamate releasing the donor acid and produces a γ -glutamyl-CoA thioester. Evidence of the existence of the γ -glutamyl-CoA thioester intermediate has been provided both by solution studies and by an X-ray crystal structure (96, 97). The acceptor substrate next binds to the enzyme and performs a nucleophilic attack on the enzyme-CoA thioester forming the second mixed anhydride. CoAS^- finally reacts with the enzyme-bound acceptor acid and the product thioester leaves.

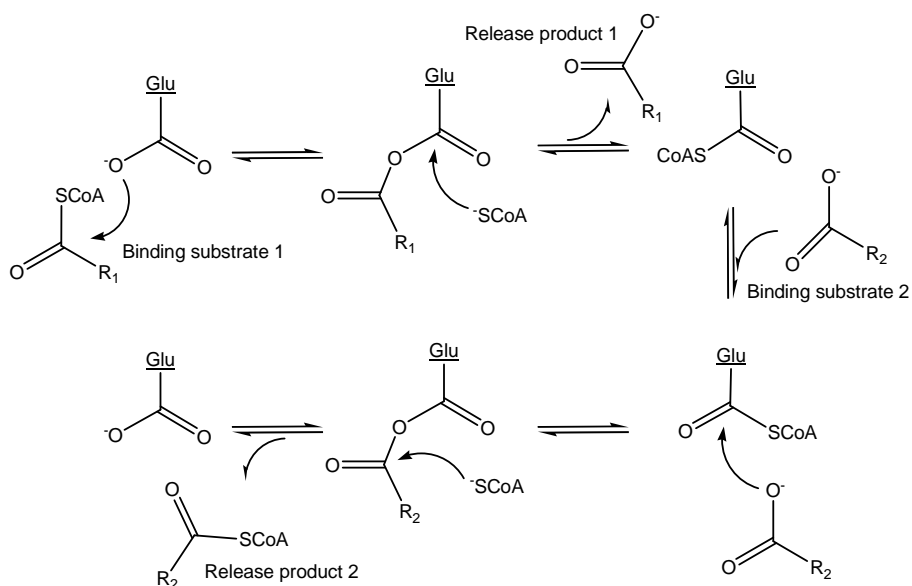


Figure 15. The catalytic mechanism of Class I CoA-transferases

3.2.2 Class II

Class II CoA-transferases catalyse a partial reaction in the multifunctional enzymes citrate or citramalate lyases. These complex enzymes consist of three subunits with different functions, a homodimeric CoA-transferase, a lyase and an acyl-carrier protein (ACP) (99). The unusual ACP contains a covalently bound dephospho-CoA derivative in the normal position of a 4'-phosphopantetheine group. The enzyme is activated by converting the thiol of the prosthetic group to an acetyl-thioester. The CoA-transferase subcomplex then catalyses the transfer of a free citrate (or citramalate) against the acyl group of ACP. The reaction mechanism differs from the Class I enzymes in that it does not involve any covalent enzyme intermediates, but proceeds through a ternary complex, where a mixed anhydride is formed between the two acids (87, 100).

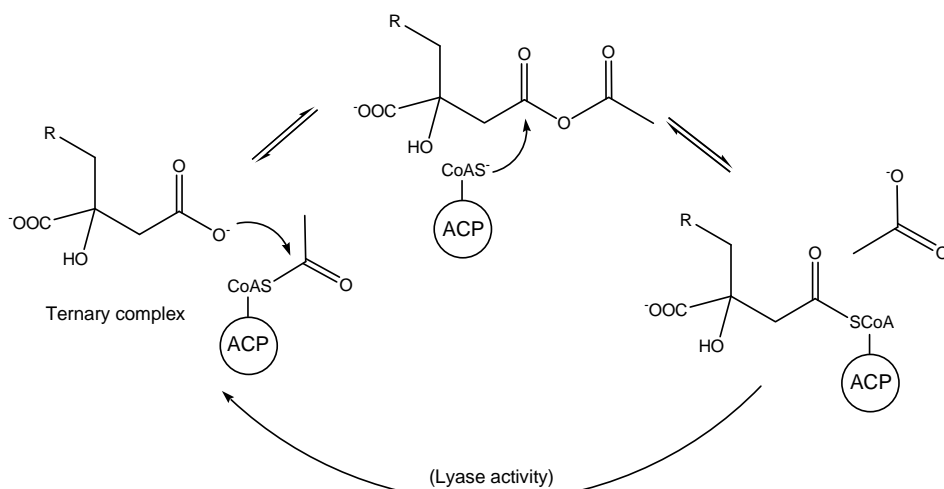


Figure 16. Catalytic mechanism by Class II CoA-transferases. R represents a carboxyl group and a hydrogen atom in citrate and citramalate, respectively.

3.2.3 Class III

The Class III is a recently identified family of CoA-transferases with most of the members from anaerobic bacteria but with also a few putative members from archaea and eukaria. Enzymes of the Class III CoA-transferases are involved in anaerobic metabolism of oxalate, carnitine, toluene and bile acid, and also in Stickland fermentation (87). Most of the members are very substrate- and stereospecific and sequence comparison show a pair-wise identity of 18-37% between them (87).

The first enzyme characterised of a Class III CoA-transferase was FRC (87), subsequently four other members of the family have been studied; the FRC ortholog in *E. coli* coded by the *yfdw* gene (YfdW) (101), γ -butyrobetaine-CoA:carnitine CoA transferase (CaiB) from *E. coli* (102, 103), succinyl-CoA:(*R*)-benzylsuccinate CoA transferase from *Thauera aromatica* (104) and (*E*)-cinnamoyl-CoA:(*R*)-phenyllactate CoA-transferase from *Clostridium sporogenes* (105). The molecular mass of the monomers range between 42 and 47 kDa and all of the members are

active as hetero- or homodimers with the exception of succinyl-CoA:(*R*)-benzylsuccinate CoA-transferase which is predicted to consist of two subunits in a $\alpha_2\beta_2$ conformation (104). It should also be noted that (*E*)-cinnamoyl-CoA:(*R*)-phenyllactate CoA transferase has been identified as part of a heterotrimeric complex, but when isolated was found to form homodimers (105).

3.2.4 Formyl-CoA transferase- Background

Very little was known about the Class III CoA-transferases prior to the crystal structure and kinetic characterisation of FRC presented in 2003 and 2004, respectively (106, 107). This section describes the knowledge about FRC and the other Class III transferases including the catalytic mechanism that was proposed for the family when the work described in pages IV and V of this thesis was initiated.

3.2.4.1 The interlocked structure of FRC

The crystal structure of FRC was ground-breaking as the first structure of any Class III CoA-transferase determined. The structure was also the first of its kind with the two 47 kDa monomers folded into rings that interlocked each other like two links of a chain. Subsequent crystal structures of YfdW (101) and CaiB (102, 103) showed this fold to not be an isolated case but a hallmark for the family.

The FRC monomer consists of a small and a large subunit connected through two long α -helical linkers. The large domain, containing both the N and C terminal parts of the protein chain, has a Rossmann-like fold with a central six-stranded parallel β -sheet flanked by helices on both sides. The small domain also has an α/β -fold but is comprised of an antiparallel three-stranded β -sheet and 6 α -helices. A large hole is formed between the two domains and the linkers connecting them (22 Å by 13 Å wide), where the second monomer is positioned in the interlaced dimer (106).

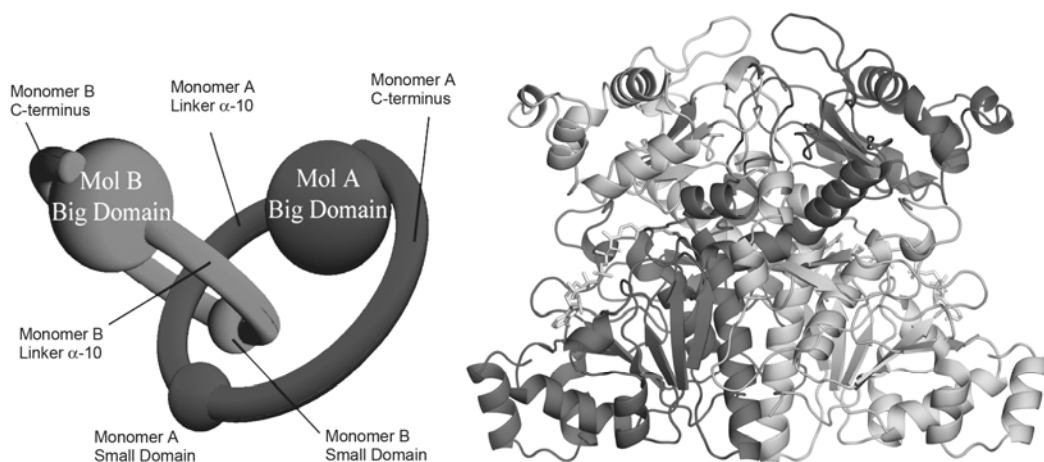


Figure 17. The schematic and crystal structure of the interlocked FRC dimer. The schematic picture is adapted from (108)

The active site of FRC was identified in a crystal structure of a complex with CoA (106). The CoA molecule binds in a cleft between the large domain of one subunit and the small domain of the other subunit. The dimeric structure thus provides two equivalent active sites. Even though the CoA binds to a Rossmann-like fold, the binding is very different from the conserved binding of NAD(P) and FAD to Rossmann folds and the thiol group faces the $\beta\alpha\beta$ -motif instead of the pyrophosphate.

3.2.4.2 Kinetic characterisation and previously proposed mechanism

Kinetic data on three of the Class III enzymes show that the catalytic mechanism is not consistent with ping-pong kinetics as observed for the Class I CoA-transferases (104, 105, 107). A conclusion from all the three studies was instead that the reaction proceeds through a ternary complex, and the mechanism was initially assumed to proceed without covalent enzyme-bound intermediates in a manner similar to that observed in the Class II CoA-transferases.

This mechanistic proposal was updated after the discovery of a covalent mixed anhydride between a conserved aspartic acid in the enzyme active site and oxalate in a structure derived from FRC co-crystallised with oxalyl-CoA (107). The new mechanism proposed still involved formation of a ternary complex, but the initial step was now an attack by the aspartic acid on the thioester resulting in the enzyme-bound aspartyl-formyl anhydride and free CoA. Next the acceptor acid would attack the mixed anhydride releasing the donor acid and the aspartyl-oxalyl anhydride would form. Finally, an attack by CoAS^- on the oxalyl moiety would release the thioester (Figure 18) (107).

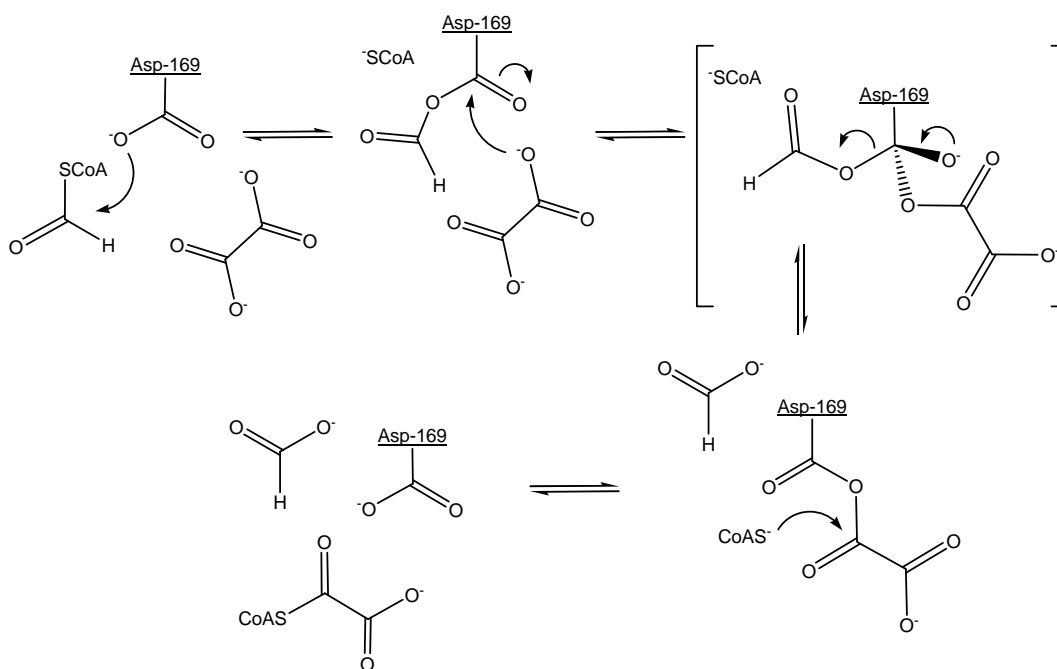


Figure 18. Previous reaction mechanism presented for FRC

Mutational studies of FRC were carried out to further substantiate the mechanistic proposal. Exchange of the aspartic acid residue for a serine or a glutamate showed to render the enzyme inactive, but surprisingly, a mutant with alanine in place of the aspartate still displayed some activity, although 1300-fold lower than for the wild-type (107). A co-crystallisation experiment of the same mutant in CaiB with both substrates also showed that the mutant retained some activity as the product was observed in the structure determined (103). Two possible scenarios were discussed to explain this finding. The first suggestion proposed was that the mechanism proceeds through an alternative mechanism in the mutant, where the donor thioester is directly attacked by the acceptor carboxylic acid (107). Secondly, a closely positioned conserved glutamic acid was assumed to substitute catalytically for the aspartate in the mutant enzyme (103).

The mechanistic proposal was soon adapted for other members of the Class III CoA-transferase family as well, but many questions remained to be answered. First of all the binding site for either acceptor or donor carboxylic acid had never been observed in any of the enzymes. An oxalate molecule was found bound in a structure of YfdW, but the position was far from the active site and the binding site was not assumed to represent the active position but a “resting” site (101). It also remained to be shown that the reaction really required a ternary complex before initiation, since the kinetic profile could result from that the donor acid remained bound to the enzyme until completion of the reaction after which both products were released at the same time.

3.3 RESULTS ON FORMYL-COENZYME A TRANSFERASE

More structural information about the catalytic steps was needed in order to further verify the mechanistic proposal for FRC. The freeze-trapping approach was therefore applied.

3.3.1 Reinvestigation of the catalytic mechanism (Paper IV)

3.3.1.1 Crystallographic identification of the β -aspartyl-CoA thioester

Crystallisation of wild-type FRC was initially carried out using conditions previously identified by S. Ricagno (109). Hanging-drop vapour diffusion experiments with a well solution containing approximately 23 % PEG 4000, 0.5 M MgCl₂ and 0.1 M HEPES buffer, pH 7.3, were set up by mixing equal volumes of the protein and well solution. Crystals belonging to the space group I4, with one dimer in the asymmetric unit grow to full size after approximately 2 days at 293 K. Freeze-trapping experiments were performed by transferring the crystals into a soak solution of a modified well solution supplemented with 10 mM formyl- or oxalyl-CoA. The crystals were picked up in cryo-loops and plunged into liquid nitrogen after incubation between 1 and 10 minutes.

Several structures were determined from crystals incubated with both formyl-CoA and oxalyl-CoA but unexpectedly they all showed to contain the same intermediate; a covalent thioester formed between the β -carboxyl group of the active site aspartate (Asp-169) and CoA. Neither formate nor oxalate could be observed in any of the structures.

Interestingly, the CoA moiety adopts different conformations in the two active sites of the dimer for all complex structures containing the β -aspartyl-CoA thioester (Figure 19). Subunit A shows the conformation of CoA previously observed in other FRC complex structures ("resting") (106, 107), while the conformation in subunit B had not been observed before ("active"). Several active site residues have changed rotamer conformation in subunit B as well. Among these is Gln-17, which in the resting active site is positioned above the enzyme-CoA thioester bond but has moved up behind Asp-169 in subunit B. A glycine-rich loop (²⁵⁸GGGGQP²⁶³) has instead closed down over the thioester bond in subunit B, in which the residue with the largest shift is positioned more than 5.5 Å away in subunit A. A 90° rotation around the C α -C β bond of Trp-48 resulting in a flip of the indole moiety is correlated with closure of the loop. Tyr-139 also shifts its side chain in order to adapt to the CoA conformations and Lys-137, Arg-38 and His-15 do so as well (Figure 19).

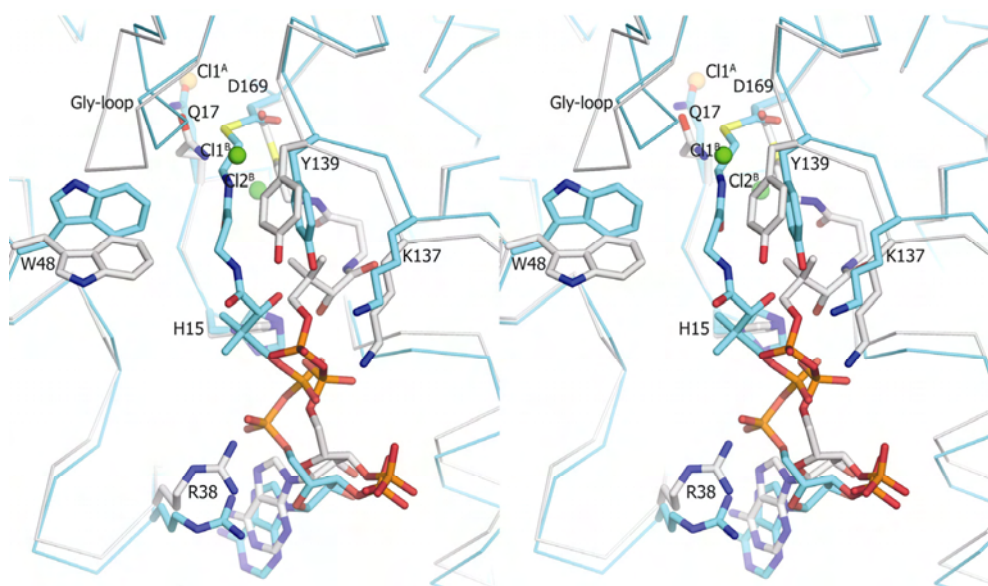


Figure 19. Stereo view of the two active sites containing the β -aspartyl-CoA thioester superimposed. Subunit A with the "resting" CoA conformation and an open glycine loop is displayed with carbon atoms in grey, while the "active" CoA molecule and the closed glycine-loop in subunit B are displayed in cyan. The chloride ion observed in the former subunit is shown in orange and the two chloride ions in the latter are shown in green

One chloride ion in subunit A and two in subunit B were modelled into the active site of the β -aspartyl-CoA thioester complexes. Kinetic measurements explained this finding, as chloride was confirmed to be a weak competitive inhibitor against oxalate and large amounts were present in the crystallisation condition. These anion binding sites were interpreted as binding sites for oxalate and formate during the catalytic reaction as will be described later on.

3.3.1.2 Identification of the β -aspartyl-CoA thioester in solution

Mass spectrometry was utilized to verify the existence of the β -aspartyl-CoA thioester also in solution. A sample of FRC incubated with formyl-CoA resulted in a main peak at 47927 ± 1 Da, which is exactly 748 Da in excess to the weight of the monomer polypeptide chain of 47196 Da (after reduction of one oxygen atom from the enzyme and one proton from CoA). No species corresponding to the apoprotein was observed (Figure 20) The experiment clearly shows that the reaction can be initiated in the absence of acceptor carboxylic acid and that it then stops at the β -aspartyl-CoA thioester.

Further confirmation of the β -aspartyl-CoA thioester existence was provided by trapping experiments with hydroxylamine and sodium borohydride. Hydroxylamine does when added to the β -aspartyl-CoA thioester intermediate form a hydroxamate at the aspartate residue while borohydride reduces aspartyl-CoA to the corresponding alcohol. Both experiments showed reduced activity of FRC when preincubated with formyl-CoA both with and without oxalate.

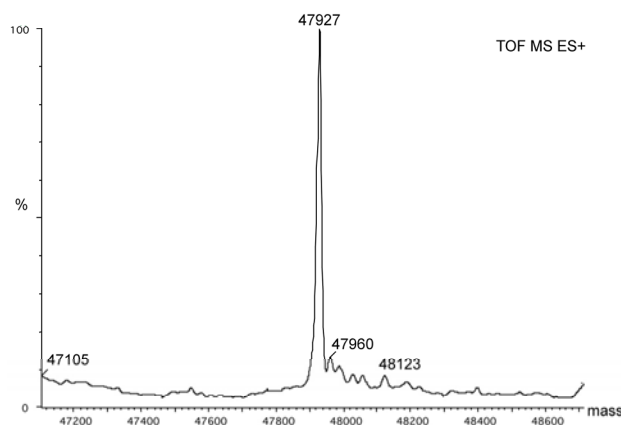


Figure 20. Mass spectrum of FRC incubated with formyl-CoA. The main species in the sample has a weight of 47927 Da which corresponds well with the mass of the enzyme-bound CoA thioester

3.3.1.3 The aspartyl-formyl anhydride

New crystallisation conditions not including chloride ions were established following the observation of the chloride ions bound in the active sites. One of the

conditions containing 1.35 M sodium citrate and 0.1 M HEPES buffer, pH 7.2-7.5, was utilized for further freeze-trapping experiments. Several attempts to transfer the crystals into a soaking solution containing the substrates were made but resulted in visually observed damage of the crystals. A new approach was therefore applied where 1 μ L at a time of a solution of 20 mM formyl-CoA in 50 mM NaAc pH 5.0 was added to the crystallisation drop. A structure containing a trapped aspartyl-formyl mixed anhydride could by this method be solved and was refined to 1.87 Å resolution. The crystal was isomorphous with previous ones and contained a dimer in the asymmetric unit. The mixed anhydride was only observed in one of the subunits of the dimer, while the other less well ordered active site displayed the enzyme-bound CoA intermediate. Superposition of the subunit with the aspartyl-formyl anhydride and the previously reported structure with the analogous aspartyl-oxalyl anhydride (107) reveals that the structures are highly similar and a notable feature in both structures is the closed glycine loop folded down protecting the anhydride.

3.3.1.4 *The Q17A and glycine loop mutants*

Of all mutant variants of FRC characterised only one amino acid except Asp-169 has shown to severely impair the catalytic activity when mutated (108). The structure of the inactive mutant enzyme Q17A was solved to 2.2 Å resolution. The dimer displays the β -aspartyl-CoA thioester in both active sites, which illustrates that the reaction can proceed until this step despite the missing glutamine residue. Both glycine loops are open in the structure and one of the subunits has an oxalate molecule bound below the loop. The position is not assumed to be the catalytic position of oxalate as both the distance and orientation are unfavourable for an attack at the β -aspartyl-CoA thioester from this site.

Two glycine loop residues, Gly-259 and Gly-260, were exchanged for alanine residues to investigate the importance of the loop for catalysis in FRC. Both mutations resulted in increased K_M values for oxalate and a crystal structure of the G260A mutant clearly showed that the conformation of the loop in neither open nor closed form could be adopted by the alanine mutant.

3.3.1.5 *Proposed catalytic mechanism*

From the identification of the β -aspartyl-CoA thioester intermediate and the complementing biochemical data we reinterpreted the catalytic mechanism in FRC (Figure 21). Based on the finding that the reaction does not require both substrates to start we concluded that formate must remain bound in the enzyme until release of oxalyl-CoA in order to obey the kinetic data (107).

The proposed scenario for catalysis in FRC, based on crystal structures and models showing important features in the active site between the catalytic steps in Figure 21, is shown in Figure 22. Formyl-CoA has in panel A been modelled into the active site where the glycine loop initially is in the open conformation. The loop then closes down during the first step of catalysis when the aspartic acid attacks the

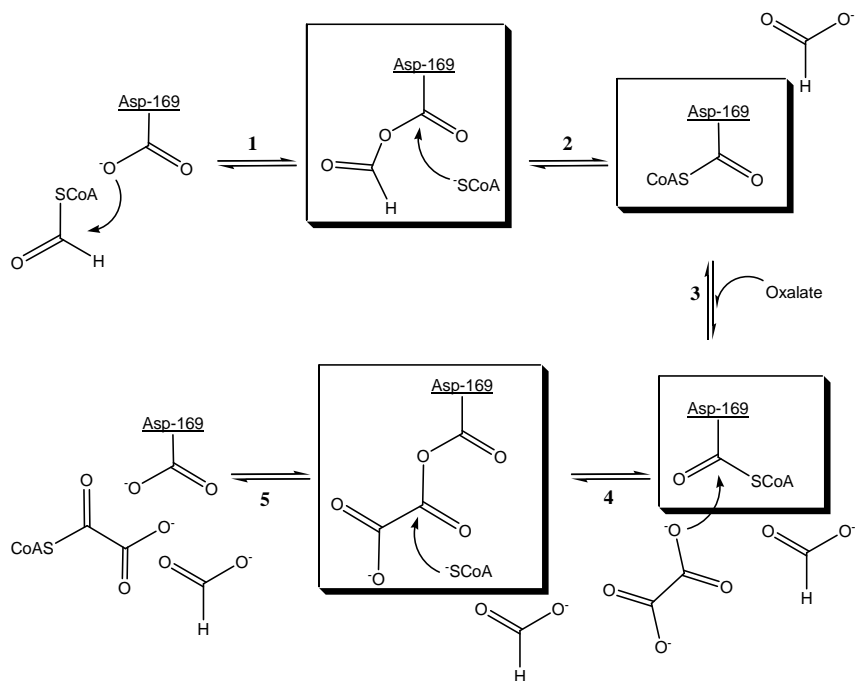


Figure 21. Proposed catalytic mechanism of FRC. Intermediates observed in crystal structures are highlighted.

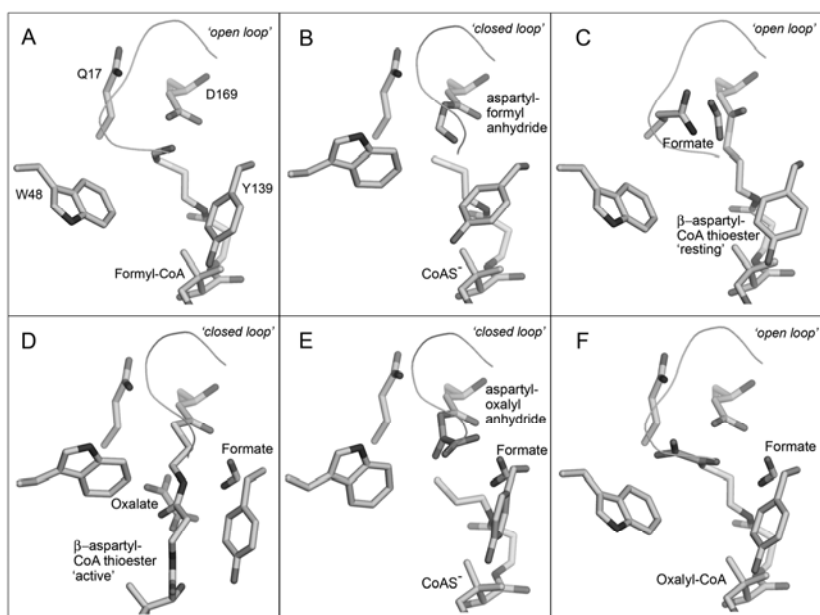


Figure 22. Models and structures of the active site between the different steps in Figure 21

formyl moiety [1] resulting in the first mixed anhydride (panel B). Next the released CoAS^- attacks the anhydride [2] and the glycine loop opens up to let the formate away. Simultaneously, Gln-17 moves down protecting the β -aspartyl-CoA thioester which now has formed (panel C). Formate has at this stage been modelled bound to the glycine loop where oxalate was observed in the Q17A mutant structure. Rearrangements of the active site are now assumed to take place [3]. The β -aspartyl-CoA thioester shifts into the "active" conformation and the glycine loop closes down moving formate down the pantetheine arm. A cavity created on the opposite side of the pantetheine with connection to the surface is interpreted as the binding site of the incoming oxalate (panel D). The formate and oxalate now bind in the two anion binding sites identified in subunit B of the β -aspartyl-CoA thioester structure, and oxalate is favourably positioned for the next nucleophilic attack on Asp-169 [4]. The second anhydride is again protected by the glycine loop (panel E) and the released CoAS^- is shifted back to the resting conformation. The final attack by CoAS^- on the oxalyl moiety [5] regenerates the aspartate residue together with oxalyl-CoA (panel F). The loop opens as the reaction is complete and the two products can leave the active site.

3.3.2 Comparison with the *E. coli* ortholog (Paper V)

The ability of *E. coli* to metabolise oxalate has not been reported, although the bacterial genome codes for close homologues of FRC and OXC. The two genes are located in an operon assumed to enhance the ability of the bacterium to survive in acidic conditions, but the function of the gene products remained to be elucidated. Kinetic characterisation of the ortholog of FRC in *E. coli*, YfdW, was carried out to verify that the putative enzyme is a formyl-CoA:oxalate transferase. The results proved this to be the case and YfdW showed to have a more than twenty times higher turnover and was more specific for the two substrates than FRC. Additionally substrate inhibition by oxalate, which was not seen for FRC, was clearly observed for YfdW.

Structural comparison of the two orthologs reveals that the active site residues are highly conserved between the two enzymes with the exception of a few residues. Trp-48, of which a 90° rotation in FRC has been shown to be correlated to the opening and closure of the glycine loop, is in YfdW replaced by a glutamine residue. However, the conserved loop (²⁴⁶GGGGQ²⁵¹ in YfdW) has been observed in both conformations in YfdW and the opening and closure is clearly not dependent on a tryptophan at this position.

Replacement of Trp-48 by a glutamine residue in FRC resulted in a mutant enzyme that exhibited substrate inhibition by oxalate. Replacement of the same residue by a phenylalanine did not have this effect. The crystal structures of the two FRC mutant variants were determined and showed that no large structural changes due to the mutations had occurred. Both structures contained the closed loop in both active sites of the dimers, and the glutamine and phenylalanine residue, respectively, adopted the same rotamer conformations as Trp-48 in case of a closed loop. The inhibition site of oxalate in W48Q FRC remains to be identified, but

interactions with the glutamine residue, and possibly also the glycine loop, are most probable.

3.3.3 Concluding remarks on formyl-CoA transferase

The existence of each of the different intermediates in Figure 21, have been experimentally verified, and we propose the modified reaction mechanism in FRC with confidence. Active site features have been summarized from all determined crystal structures and a catalytic scenario has been concluded by combining these. The crystal structures determined in the presence of chloride ions resulted in identification of possible anion binding sites for the carboxylic acids substrate and product, and a new intermediate in the reaction path could be observed.

Whether or not the reaction mechanism for FRC can be applied to other members of the Class III CoA-transferase family has not yet been investigated. The glycine-rich loop has not been observed as a conserved feature in homologues of FRC. Interestingly, a domain movement upon CoA binding was identified in CaiB (102, 103). The domain movement has been speculated to be a different mode of shielding the active site when larger acyl groups are to be transferred (102).

The role of the FRC and OXC homologues in *E. coli* remains to be established. But we observe that YfdW is more substrate specific and efficient than FRC and its coupled action with the putative decarboxylase could by the consumption of one proton per oxalate turned over help the bacteria to survive under acidic conditions. A buffering effect by the released carbon dioxide could also be speculated.

Replacement of a single tryptophan residue in the active site of FRC with the cognate glutamine residue in YfdW led to a substrate specificity resembling that of YfdW. The replacement further showed that the tryptophan residue precludes substrate inhibition in FRC, which was observed in YfdW and the glutamine mutant variant of FRC.

4 REFERENCES

1. H. E. Williams and L. H. Smith, Jr. (1968) Disorders of oxalate metabolism. *Am J Med* **45**(5), 715-35
2. A. Hodgkinson. (1977) *Oxalic Acid in Biology and Medicine*, Academic Press Inc. (London) Ltd.
3. L. F. James. (1972) Oxalate toxicosis. *Clin Toxicol* **5**(2), 231-43
4. R. A. Rodby, T. S. Tyszka and J. W. Williams. (1991) Reversal of cardiac dysfunction secondary to type 1 primary hyperoxaluria after combined liver-kidney transplantation. *Am J Med* **90**(4), 498-504
5. M. Hatch, R. W. Freel and N. D. Vaziri. (1994) Mechanisms of oxalate absorption and secretion across the rabbit distal colon. *Pflugers Arch* **426**(1-2), 101-9
6. M. J. Allison, H. M. Cook, D. B. Milne, S. Gallagher and R. V. Clayman. (1986) Oxalate degradation by gastrointestinal bacteria from humans. *J Nutr* **116**(3), 455-60
7. M. J. Allison, K. A. Dawson, W. R. Mayberry and J. G. Foss. (1985) *Oxalobacter formigenes* gen. nov., sp. nov.: oxalate-degrading anaerobes that inhabit the gastrointestinal tract. *Arch Microbiol* **141**(1), 1-7
8. M. Hatch and R. W. Freel. (2005) Intestinal transport of an obdurate anion: oxalate. *Urol Res* **33**(1), 1-16
9. H. Sidhu, M. E. Schmidt, J. G. Cornelius, S. Thamilselvan, S. R. Khan, A. Hesse and A. B. Peck. (1999) Direct correlation between hyperoxaluria/oxalate stone disease and the absence of the gastrointestinal tract-dwelling bacterium *Oxalobacter formigenes*: possible prevention by gut recolonization or enzyme replacement therapy. *J Am Soc Nephrol* **10 Suppl 14**, S334-40
10. J. G. Cornelius and A. B. Peck. (2004) Colonization of the neonatal rat intestinal tract from environmental exposure to the anaerobic bacterium *Oxalobacter formigenes*. *J Med Microbiol* **53**(Pt 3), 249-54
11. S. H. Duncan, A. J. Richardson, P. Kaul, R. P. Holmes, M. J. Allison and C. S. Stewart. (2002) *Oxalobacter formigenes* and its potential role in human health. *Appl Environ Microbiol* **68**(8), 3841-7
12. B. Hoppe, B. Beck, N. Gatter, G. von Unruh, A. Tischer, A. Hesse, N. Laube, P. Kaul and H. Sidhu. (2006) *Oxalobacter formigenes*: a potential tool for the treatment of primary hyperoxaluria type 1. *Kidney Int* **70**(7), 1305-11
13. V. Anantharam, M. J. Allison and P. C. Maloney. (1989) Oxalate:formate exchange. The basis for energy coupling in *Oxalobacter*. *J Biol Chem* **264**(13), 7244-50
14. Z. S. Ruan, V. Anantharam, I. T. Crawford, S. V. Ambudkar, S. Y. Rhee, M. J. Allison and P. C. Maloney. (1992) Identification, purification, and reconstitution of OxIT, the oxalate: formate antiport protein of *Oxalobacter formigenes*. *J Biol Chem* **267**(15), 10537-43

15. T. Hirai, J. A. Heymann, D. Shi, R. Sarker, P. C. Maloney and S. Subramaniam. (2002) Three-dimensional structure of a bacterial oxalate transporter. *Nat Struct Biol* **9**(8), 597-600
16. J. A. Heymann, T. Hirai, D. Shi and S. Subramaniam. (2003) Projection structure of the bacterial oxalate transporter OxIT at 3.4Å resolution. *J Struct Biol* **144**(3), 320-6
17. A. L. Baetz and M. J. Allison. (1989) Purification and characterization of oxalyl-coenzyme A decarboxylase from *Oxalobacter formigenes*. *J Bacteriol* **171**(5), 2605-8
18. A. L. Baetz and M. J. Allison. (1990) Purification and characterization of formyl-coenzyme A transferase from *Oxalobacter formigenes*. *J Bacteriol* **172**(7), 3537-40
19. A. L. Baetz and M. J. Allison. (1992) Localization of oxalyl-CoA decarboxylase and formyl-CoA transferase in *Oxalobacter formigenes* cells. *Syst. Appl. Microbiol.* **15**, 167-71
20. N. A. Cornick and M. J. Allison. (1996) Anabolic Incorporation of Oxalate by *Oxalobacter formigenes*. *Appl Environ Microbiol* **62**(8), 3011-3
21. R. F. Butterworth. (2006) *Modern Nutrition in Health and Disease*, 10 Ed., Lippincott Williams & Wilkins, Baltimore
22. R. J. Williams, W. A. Mosher and E. Rohrman. (1936) The importance of "pantothenic acid" in fermentation, respiration and glycogen storage. *Biochem J* **30**(11), 2036-9
23. F. Jordan. (2003) Current mechanistic understanding of thiamin diphosphate-dependent enzymatic reactions. *Nat Prod Rep* **20**(2), 184-201
24. A. Schellenberger. (1998) Sixty years of thiamin diphosphate biochemistry. *Biochim Biophys Acta* **1385**(2), 177-86
25. D. Kern, G. Kern, H. Neef, K. Tittmann, M. Killenberg-Jabs, C. Wikner, G. Schneider and G. Hubner. (1997) How thiamine diphosphate is activated in enzymes. *Science* **275**(5296), 67-70
26. F. Jordan and Y. H. Mariam. (1978) N1'-Methylthiaminium Diiodide. Model study on the effect of a coenzyme bound positive charge reaction mechanism requiring thiamin pyrophosphate. *J Am Chem Soc* **100**(8), 2534-41
27. G. Schneider and Y. Lindqvist. (1993) Enzymatic thiamine catalysis: mechanistic implications from the three-dimensional structure of transketolase. *Bioorg. Chem.* **21**, 109-17
28. M. W. Washabaugh and W. P. Jencks. (1988) Thiazolium C(2)-proton exchange: structure-reactivity correlations and the pKa of thiamin C(2)-H revisited. *Biochemistry* **27**(14), 5044-53
29. Y. Lindqvist, G. Schneider, U. Ermler and M. Sundstrom. (1992) Three-dimensional structure of transketolase, a thiamine diphosphate dependent enzyme, at 2.5 Å resolution. *Embo J* **11**(7), 2373-9
30. Y. A. Muller and G. E. Schulz. (1993) Structure of the thiamine- and flavin-dependent enzyme pyruvate oxidase. *Science* **259**(5097), 965-7

31. F. Dyda, W. Furey, S. Swaminathan, M. Sax, B. Farrenkopf and F. Jordan. (1993) Catalytic centers in the thiamin diphosphate dependent enzyme pyruvate decarboxylase at 2.4-Å resolution. *Biochemistry* **32**(24), 6165-70
32. D. Dobritzsch, S. König, G. Schneider and G. Lu. (1998) High resolution crystal structure of pyruvate decarboxylase from *Zymomonas mobilis*. Implications for substrate activation in pyruvate decarboxylases. *J Biol Chem* **273**(32), 20196-204
33. A. Schutz, T. Sandalova, S. Ricagno, G. Hubner, S. König and G. Schneider. (2003) Crystal structure of thiamindiphosphate-dependent indolepyruvate decarboxylase from *Enterobacter cloacae*, an enzyme involved in the biosynthesis of the plant hormone indole-3-acetic acid. *Eur J Biochem* **270**(10), 2312-21
34. M. S. Hasson, A. Muscate, M. J. McLeish, L. S. Polovnikova, J. A. Gerlt, G. L. Kenyon, G. A. Petsko and D. Ringe. (1998) The crystal structure of benzoylformate decarboxylase at 1.6 Å resolution: diversity of catalytic residues in thiamin diphosphate-dependent enzymes. *Biochemistry* **37**(28), 9918-30
35. C. L. Berthold, P. Moussatche, N. G. Richards and Y. Lindqvist. (2005) Structural basis for activation of the thiamin diphosphate-dependent enzyme oxalyl-CoA decarboxylase by adenosine diphosphate. *J Biol Chem* **280**(50), 41645-54
36. S. S. Pang, R. G. Duggleby and L. W. Guddat. (2002) Crystal structure of yeast acetohydroxyacid synthase: a target for herbicidal inhibitors. *J Mol Biol* **317**(2), 249-62
37. S. S. Pang, R. G. Duggleby, R. L. Schowen and L. W. Guddat. (2004) The crystal structures of *Klebsiella pneumoniae* acetolactate synthase with enzyme-bound cofactor and with an unusual intermediate. *J Biol Chem* **279**(3), 2242-53
38. T. G. Mosbacher, M. Mueller and G. E. Schulz. (2005) Structure and mechanism of the ThDP-dependent benzaldehyde lyase from *Pseudomonas fluorescens*. *Febs J* **272**(23), 6067-76
39. M. E. Caines, J. M. Elkins, K. S. Hewitson and C. J. Schofield. (2004) Crystal structure and mechanistic implications of N²-(2-carboxyethyl)arginine synthase, the first enzyme in the clavulanic acid biosynthesis pathway. *J Biol Chem* **279**(7), 5685-92
40. W. Versees, S. Spaepen, J. Vanderleyden and J. Steyaert. (2007) The crystal structure of phenylpyruvate decarboxylase from *Azospirillum brasilense* at 1.5 Å resolution. Implications for its catalytic and regulatory mechanism. *Febs J* **274**(9), 2363-75
41. C. L. Berthold, D. Gocke, M. D. Wood, F. Leeper, M. Pohl and G. Schneider. (2007) Structure of the branched-chain keto acid decarboxylase (KdcA) from *Lactococcus lactis* provides insights into the structural basis for the chemoselective and enantioselective carbonylation reaction *Acta Crystallogr.* **D63**(12), 1217-24
42. S. Xiang, G. Usunow, G. Lange, M. Busch and L. Tong. (2007) Crystal structure of 1-deoxy-D-xylulose 5-phosphate synthase, a crucial enzyme for isoprenoids biosynthesis. *J Biol Chem* **282**(4), 2676-82

43. E. Chabriere, M. H. Charon, A. Volbeda, L. Pieulle, E. C. Hatchikian and J. C. Fontecilla-Camps. (1999) Crystal structures of the key anaerobic enzyme pyruvate:ferredoxin oxidoreductase, free and in complex with pyruvate. *Nat Struct Biol* **6**(2), 182-90
44. P. Arjunan, N. Nemeria, A. Brunskill, K. Chandrasekhar, M. Sax, Y. Yan, F. Jordan, J. R. Guest and W. Furey. (2002) Structure of the pyruvate dehydrogenase multienzyme complex E1 component from *Escherichia coli* at 1.85 Å resolution. *Biochemistry* **41**(16), 5213-21
45. E. M. Ciszak, L. G. Korotchkina, P. M. Dominiak, S. Sidhu and M. S. Patel. (2003) Structural basis for flip-flop action of thiamin pyrophosphate-dependent enzymes revealed by human pyruvate dehydrogenase. *J Biol Chem* **278**(23), 21240-6
46. R. A. Frank, A. J. Price, F. D. Northrop, R. N. Perham and B. F. Luisi. (2007) Crystal structure of the E1 component of the *Escherichia coli* 2-oxoglutarate dehydrogenase multienzyme complex. *J Mol Biol* **368**(3), 639-51
47. A. Ævarsson, J. L. Chuang, R. M. Wynn, S. Turley, D. T. Chuang and W. G. Hol. (2000) Crystal structure of human branched-chain alpha-ketoacid dehydrogenase and the molecular basis of multienzyme complex deficiency in maple syrup urine disease. *Structure* **8**(3), 277-91
48. A. Ævarsson, K. Seger, S. Turley, J. R. Sokatch and W. G. Hol. (1999) Crystal structure of 2-oxoisovalerate dehydrogenase and the architecture of 2-oxo acid dehydrogenase multienzyme complexes. *Nat Struct Biol* **6**(8), 785-92
49. T. Nakai, N. Nakagawa, N. Maoka, R. Masui, S. Kuramitsu and N. Kamiya. (2004) Ligand-induced conformational changes and a reaction intermediate in branched-chain 2-oxo acid dehydrogenase (E1) from *Thermus thermophilus* HB8, as revealed by X-ray crystallography. *J Mol Biol* **337**(4), 1011-33
50. J. Li, M. Machius, J. L. Chuang, R. M. Wynn and D. T. Chuang. (2007) The two active sites in human branched-chain alpha-keto acid dehydrogenase operate independently without an obligatory alternating-site mechanism. *J Biol Chem* **282**(16), 11904-13
51. M. Pohl, G. A. Sprenger and M. Muller. (2004) A new perspective on thiamine catalysis. *Curr Opin Biotechnol* **15**(4), 335-42
52. E. C. Heath, J. Hurwitz, B. L. Horecker and A. Ginsburg. (1958) Pentose fermentation by *Lactobacillus plantarum*. I. The cleavage of xylulose 5-phosphate by phosphoketolase. *J Biol Chem* **231**(2), 1009-29
53. Y. Sakai, T. Nakagawa, M. Shimase and N. Kato. (1998) Regulation and physiological role of the DAS1 gene, encoding dihydroxyacetone synthase, in the methylotrophic yeast *Candida boidinii*. *J Bacteriol* **180**(22), 5885-90
54. Y. A. Muller, Y. Lindqvist, W. Furey, G. E. Schulz, F. Jordan and G. Schneider. (1993) A thiamin diphosphate binding fold revealed by comparison of the crystal structures of transketolase, pyruvate oxidase and pyruvate decarboxylase. *Structure* **1**(2), 95-103
55. R. G. Duggleby. (2006) Domain relationships in thiamine diphosphate-dependent enzymes. *Acc Chem Res* **39**(8), 550-7

56. R. A. Laskowski, V. V. Chistyakov and J. M. Thornton. (2005) PDBsum more: new summaries and analyses of the known 3D structures of proteins and nucleic acids. *Nucleic Acids Res* **33**(Database issue), D266-8
57. Y. Y. Chang, A. Y. Wang and J. E. Cronan, Jr. (1993) Molecular cloning, DNA sequencing, and biochemical analyses of *Escherichia coli* glyoxylate carboligase. An enzyme of the acetohydroxy acid synthase-pyruvate oxidase family. *J Biol Chem* **268**(6), 3911-9
58. J. Kim, D. G. Beak, Y. T. Kim, J. D. Choi and M. Y. Yoon. (2004) Effects of deletions at the C-terminus of tobacco acetohydroxyacid synthase on the enzyme activity and cofactor binding. *Biochem J* **384**(Pt 1), 59-68
59. C. L. Berthold, C. G. Toyota, P. Moussatche, M. D. Wood, F. Leeper, N. G. Richards and Y. Lindqvist. (2007) Crystallographic snapshots of oxalyl-CoA decarboxylase give insights into catalysis by nonoxidative ThDP-dependent decarboxylases. *Structure* **15**(7), 853-61
60. C. F. Hawkins, A. Borges and R. N. Perham. (1989) A common structural motif in thiamin pyrophosphate-binding enzymes. *FEBS Lett* **255**(1), 77-82
61. W. Shin, J. Pletcher, G. Blank and M. Sax. (1977) Ring stacking interactions between thiamin and planar molecules as seen in the crystal structure of a thiamin picrolonate dihydrate complex. *J Am Chem Soc* **99**(10), 3491-9
62. F. Jordan. (1974) Semiempirical calculations on the electronic structure and preferred conformations of thiamine (vitamin B1) and thiamine pyrophosphate (cocarboxylase). *J Am Chem Soc* **96**(11), 3623-30
63. F. Jordan. (1976) Theoretical calculations on thiamine and related compounds. II. Conformational analysis and electronic properties of 2-(alpha-hydroxyethyl)thiamine. *J Am Chem Soc* **98**(3), 808-13
64. F. Guo, D. Zhang, A. Kahyaoglu, R. S. Farid and F. Jordan. (1998) Is a hydrophobic amino acid required to maintain the reactive V conformation of thiamin at the active center of thiamin diphosphate-requiring enzymes? Experimental and computational studies of isoleucine 415 of yeast pyruvate decarboxylase. *Biochemistry* **37**(38), 13379-91
65. N. Nemeria, S. Chakraborty, A. Baykal, L. G. Korotchkina, M. S. Patel and F. Jordan. (2007) The 1',4'-iminopyrimidine tautomer of thiamin diphosphate is poised for catalysis in asymmetric active centers on enzymes. *Proc Natl Acad Sci U S A* **104**(1), 78-82
66. C. Wikner, L. Meshalkina, U. Nilsson, M. Nikkola, Y. Lindqvist, M. Sundstrom and G. Schneider. (1994) Analysis of an invariant cofactor-protein interaction in thiamin diphosphate-dependent enzymes by site-directed mutagenesis. Glutamic acid 418 in transketolase is essential for catalysis. *J Biol Chem* **269**(51), 32144-50
67. J. M. Candy, J. Koga, P. F. Nixon and R. G. Duggleby. (1996) The role of residues glutamate-50 and phenylalanine-496 in *Zymomonas mobilis* pyruvate decarboxylase. *Biochem J* **315** (Pt 3), 745-51
68. M. Killenberg-Jabs, S. Konig, I. Eberhardt, S. Hohmann and G. Hubner. (1997) Role of Glu51 for cofactor binding and catalytic activity in pyruvate decarboxylase from yeast studied by site-directed mutagenesis. *Biochemistry* **36**(7), 1900-5

69. A. Bar-Ilan, V. Balan, K. Tittmann, R. Golbik, M. Vyazmensky, G. Hubner, Z. Barak and D. M. Chipman. (2001) Binding and activation of thiamin diphosphate in acetohydroxyacid synthase. *Biochemistry* **40**(39), 11946-54
70. R. Fang, P. F. Nixon and R. G. Duggleby. (1998) Identification of the catalytic glutamate in the E1 component of human pyruvate dehydrogenase. *FEBS Lett* **437**(3), 273-7
71. Q. Hu and R. Kluger. (2004) Fragmentation of the conjugate base of 2-(1-hydroxybenzyl)thiamin: does benzoylformate decarboxylase prevent orbital overlap to avoid it? *J Am Chem Soc* **126**(1), 68-9
72. E. S. Polovnikova, M. J. McLeish, E. A. Sergienko, J. T. Burgner, N. L. Anderson, A. K. Bera, F. Jordan, G. L. Kenyon and M. S. Hasson. (2003) Structural and kinetic analysis of catalysis by a thiamin diphosphate-dependent enzyme, benzoylformate decarboxylase. *Biochemistry* **42**(7), 1820-30
73. G. Schenk, F. J. Leeper, R. England, P. F. Nixon and R. G. Duggleby. (1997) The role of His113 and His114 in pyruvate decarboxylase from *Zymomonas mobilis*. *Eur J Biochem* **248**(1), 63-71
74. A. T. Brünger, P. D. Adams, G. M. Clore, W. L. DeLano, P. Gros, R. W. Grosse-Kunstleve, J. S. Jiang, J. Kuszewski, M. Nilges, N. S. Pannu, R. J. Read, L. M. Rice, T. Simonson and G. L. Warren. (1998) Crystallography & NMR system: A new software suite for macromolecular structure determination. *Acta Crystallogr.* **D54 (Pt 5)**, 905-21
75. S. Mann, C. Perez Melero, D. Hawksley and F. J. Leeper. (2004) Inhibition of thiamin diphosphate dependent enzymes by 3-deazathiamin diphosphate. *Org Biomol Chem* **2**(12), 1732-41
76. F. J. Leeper, D. Hawksley, S. Mann, C. Perez Melero and M. D. Wood. (2005) Studies on thiamine diphosphate-dependent enzymes. *Biochem Soc Trans* **33**(Pt 4), 772-5
77. M. Machius, R. M. Wynn, J. L. Chuang, J. Li, R. Kluger, D. Yu, D. R. Tomchick, C. A. Brautigam and D. T. Chuang. (2006) A versatile conformational switch regulates reactivity in human branched-chain alpha-ketoacid dehydrogenase. *Structure* **14**(2), 287-98
78. D. Voet, J. G. Voet and C. W. Pratt. (1999) *Fundamentals of biochemistry*, John Wiley & Sons, New York
79. F. Lipmann. (1945) Acetylation of sulfanilamide by liver homogenates and extracts. *J. Biol. Chem.* **160**(1), 173-90
80. T. Brody. (1999) *Nutritional Biochemistry*, 2nd Ed., Academic Press, San Diego
81. P. K. Mishra and D. G. Drueckhammer. (2000) Coenzyme A Analogues and Derivatives: Synthesis and Applications as Mechanistic Probes of Coenzyme A Ester-Utilizing Enzymes. *Chem Rev* **100**(9), 3283-310
82. P. R. Trumbo. (2006) *Modern Nutrition in Health and Disease*, 10 Ed., Lippincott Williams & Wilkins, Baltimore
83. J. Baddiley, E. M. Thain, G. D. Novelli and F. Lipmann. (1953) Structure of coenzyme A. *Nature* **171**(4341), 76

84. C. Engel and R. Wierenga. (1996) The diverse world of coenzyme A binding proteins. *Curr Opin Struct Biol* **6**(6), 790-7
85. M. G. Rossmann, A. Liljas, C. I. Brändén and L. Banaszak. (1975) *The Enzymes*, Academic Press, New York
86. M. Saraste, P. R. Sibbald and A. Wittinghofer. (1990) The P-loop-a common motif in ATP- and GTP-binding proteins. *Trends Biochem Sci* **15**(11), 430-4
87. J. Heider. (2001) A new family of CoA-transferases. *FEBS Lett* **509**(3), 345-9
88. H. White and W. P. Jencks. (1976) Mechanism and specificity of succinyl-CoA:3-ketoacid coenzyme A transferase. *J Biol Chem* **251**(6), 1688-99
89. I. E. Corthesy-Theulaz, G. E. Bergonzelli, H. Henry, D. Bachmann, D. F. Schorderet, A. L. Blum and L. N. Ornston. (1997) Cloning and characterization of *Helicobacter pylori* succinyl CoA:acetoacetate CoA-transferase, a novel prokaryotic member of the CoA-transferase family. *J Biol Chem* **272**(41), 25659-67
90. R. E. Parales and C. S. Harwood. (1992) Characterization of the genes encoding beta-ketoadipate: succinyl-coenzyme A transferase in *Pseudomonas putida*. *J Bacteriol* **174**(14), 4657-66
91. D. P. Wiesenborn, F. B. Rudolph and E. T. Papoutsakis. (1989) Coenzyme A transferase from *Clostridium acetobutylicum* ATCC 824 and its role in the uptake of acids. *Appl Environ Microbiol* **55**(2), 323-9
92. H. A. Barker, I. M. Jeng, N. Neff, J. M. Robertson, F. K. Tam and S. Hosaka. (1978) Butyryl-CoA:acetoacetate CoA-transferase from a lysine-fermenting *Clostridium*. *J Biol Chem* **253**(4), 1219-25
93. K. S. Bateman, E. R. Brownie, W. T. Wolodko and M. E. Fraser. (2002) Structure of the mammalian CoA transferase from pig heart. *Biochemistry* **41**(49), 14455-62
94. W. Buckel, U. Dorn and R. Semmler. (1981) Glutaconate CoA-transferase from *Acidaminococcus fermentans*. *Eur J Biochem* **118**(2), 315-21
95. U. Jacob, M. Mack, T. Clausen, R. Huber, W. Buckel and A. Messerschmidt. (1997) Glutaconate CoA-transferase from *Acidaminococcus fermentans*: the crystal structure reveals homology with other CoA-transferases. *Structure* **5**(3), 415-26
96. E. S. Rangarajan, Y. Li, E. Ajamian, P. Iannuzzi, S. D. Kernaghan, M. E. Fraser, M. Cygler and A. Matte. (2005) Crystallographic trapping of the glutamyl-CoA thioester intermediate of family I CoA transferases. *J Biol Chem* **280**(52), 42919-28
97. F. Solomon and W. P. Jencks. (1969) Identification of an enzyme-gamma-glutamyl coenzyme A intermediate from coenzyme A transferase. *J Biol Chem* **244**(3), 1079-81
98. T. Selmer and W. Buckel. (1999) Oxygen exchange between acetate and the catalytic glutamate residue in glutaconate CoA-transferase from *Acidaminococcus fermentans*. Implications for the mechanism of CoA-ester hydrolysis. *J Biol Chem* **274**(30), 20772-8

99. P. Dimroth and H. Eggerer. (1975) Isolation of subunits of citrate lyase and characterization of their function in the enzyme complex. *Proc Natl Acad Sci U S A* **72**(9), 3458-62
100. W. Buckel and A. Bobi. (1976) The enzyme complex citramalate lyase from *Clostridium tetanomorphum*. *Eur J Biochem* **64**(1), 255-62
101. A. Gruez, V. Roig-Zamboni, C. Valencia, V. Campanacci and C. Cambillau. (2003) The crystal structure of the *Escherichia coli* YfdW gene product reveals a new fold of two interlaced rings identifying a wide family of CoA transferases. *J Biol Chem* **278**(36), 34582-6
102. P. Stenmark, D. Gurmu and P. Nordlund. (2004) Crystal structure of CaiB, a type-III CoA transferase in carnitine metabolism. *Biochemistry* **43**(44), 13996-4003
103. E. S. Rangarajan, Y. Li, P. Iannuzzi, M. Cygler and A. Matte. (2005) Crystal structure of *Escherichia coli* crotonobetainyl-CoA: carnitine CoA-transferase (CaiB) and its complexes with CoA and carnitiny-CoA. *Biochemistry* **44**(15), 5728-38
104. C. Leutwein and J. Heider. (2001) Succinyl-CoA:(R)-benzylsuccinate CoA-transferase: an enzyme of the anaerobic toluene catabolic pathway in denitrifying bacteria. *J Bacteriol* **183**(14), 4288-95
105. S. Dickert, A. J. Pierik, D. Linder and W. Buckel. (2000) The involvement of coenzyme A esters in the dehydration of (R)-phenyllactate to (E)-cinnamate by *Clostridium sporogenes*. *Eur J Biochem* **267**(12), 3874-84
106. S. Ricagno, S. Jonsson, N. Richards and Y. Lindqvist. (2003) Formyl-CoA transferase encloses the CoA binding site at the interface of an interlocked dimer. *Embo J* **22**(13), 3210-9
107. S. Jonsson, S. Ricagno, Y. Lindqvist and N. G. Richards. (2004) Kinetic and mechanistic characterization of the formyl-CoA transferase from *Oxalobacter formigenes*. *J Biol Chem* **279**(34), 36003-12
108. S. Ricagno. (2004) in PhD thesis *Formyl-Coenzyme A transferase, structure and enzymatic mechanism*. Department of medical biochemistry and biophysics, Karolinska Institutet Stockholm
109. S. Ricagno, S. Jonsson, N. Richards and Y. Lindqvist. (2003) Crystallization and preliminary crystallographic analysis of formyl-CoA transferase from *Oxalobacter formigenes*. *Acta Crystallogr D Biol Crystallogr* **59**(Pt 7), 1276-7

5 ACKNOWLEDGEMENTS

There are many people I would like to thank for their contributions to the work presented in this thesis, but also for other inspiring collaborations during the time of my PhD studies.

First of all I would like to thank my supervisors Prof. Ylva Lindqvist and Prof. Gunter Schneider for guiding me with your scientific knowledge and continuous support throughout the years. It has been encouraging to see how you meet challenging scientific questions with enthusiasm. Many thanks also for all the nice dinners at your place. I especially enjoyed Gunter's cooking and the company of interesting scientists from all over the world.

I would also like to express my sincere gratitude to the *Oxalobacter* collaborators at the University of Florida, Prof. Nigel G.J. Richards, Cory Toyota and Patricia Moussatche. A special thank to Nigel and Cory for your support and excellent contributions during the very hectic final half a year.

Thank you Dörte Gocke and Martina Pohl at the research centre in Jülich for introducing me to several new enzymes and a very fruitful collaboration. Dörte, I really enjoyed working with you, and it is a pleasure for a crystallographer to be provided with grams of ultrapure protein!

I have spent many days (and nights) during the last 4 years at the synchrotrons. Thank you, Tanja and Doreen, for teaching me a lot about data collection and processing. One of my strongest memories so far from my scientific career is from the ESRF when we saw the first high-resolution diffraction from an OXC crystal. Robert, I truly enjoyed all our discussions, both at the beamlines after too little sleep but also during normal days in the lab. Jodie as one of my constant friends at the synchrotron and in the lab, thank you for sharing successful trips as well as times when hope was almost lost. Your proof-reading of manuscripts and thesis, and guidance with the scientific English has helped me enormously.

Stina, who has been with me during all the years, thank you for all your support and understanding. It has been encouraging to write the thesis in parallel with you. Daniel, also a friend during all these years, I really enjoyed our work together. Hanna, as the friendliest and most happy colleague one can have, your optimism has often helped to cheer me up. Magnus, my "next bench" mate in the lab, sorry for talking too much while you were pipetting and thank you for being my "living dictionary". Edvard, thank you for being so relaxed and always very kind.

Thank you Eva, for taking care of everything and organising things so well. Ahmad (and previously also Mona), without you the lab would not run, thank you. Jean-Marie, every group needs a French man. Jola, Inari, Laura, Mikko and Maria, thank you all for a nice time in the group, at coffee as well as during scientific discussions.

There are several former members of the lab I would like to express my gratefulness to as well. First of all Stefano for taking care of me when I first came to the group, and for introducing me to the project. Thank you also to Azmiri, my long time room-mate and company for many conferences. Bernie, thank you for crystallographic expertise and introducing Coot. Anna, Lucas, Jenny and Martin, now I know what you went through stuck in front of the computer writing your theses.

Under åren har jag även fått mycket support utanför arbetet. Tack till alla mina underbara vänner, hoppas jag inte tråkat ut er. Läs den här boken, så förstår ni vad jag arbetat med under de senaste åren (eller kanske inte).

Tack till Jespers (och snart min) familj som följt mitt forskande med stort intresse. Min bror Rickard och Marie, snart lovar jag att bjuda på fler middagar igen.

Slutligen, vill jag tacka min underbara mamma och pappa, tack för er omtanke och att ni verkligen alltid ställer upp.

Tack Jesper, för allt.